1 **Histamine Type 1-Receptor activation by low dose of histamine undermines human**

2 **Glomerular Slit Diaphragm Integrity**

3 *Eleonora Veglia[a#], Alessandro Pini[b#]*, Aldo Moggio[a1], Cristina Grange[c], Federica Premoselli[d],*

4 *Gianluca Miglio[a], Katerina Tiligada[e] Roberto Fantozzi[a], Paul L. Chazot[f], Arianna Carolina Rosa[a,f]*

5

6 [#]*Authors contributed equally to this work*

7 [a]*Department of Scienza e Tecnologia del Farmaco, University of Turin, Via P. Giuria 9 - 10125,*

8 *Turin, Italy, eveglia@unito.it, aldomoggio@gmail.com, rfantozzi@unito.it, acrosa@unito.it;*

9 [b]*Department of Clinical and Experimental Medicine, University of Florence, Viale Pieraccini 6 -*

10 *50139, Florence, Italy, apini@unito.it;* [c]*Department of Scienze Mediche, University of Turin, C.So*

11 *Dogliotti 14 - 10126 Turin, Italy, cgrange@unito.it;* [d]*Department of Neuroscience "Rita Levi*

12 *Montalcini", University of Turin, Via Cherasco 15, 10126 Turin, Italy, fpremoselli@unito.it;*

13 [e]*Department of Pharmacology, Medical School, University of Athens, M. Asias 75 GR-115 27*

14 *Athens, Greece, aityliga@med.uoa.gr;* [f]*School of Biological and Biomedical Science, Durham*

15 *University, Durham DH13LE, UK, paul.chazot@durham.ac.uk*

16

17 ***Corresponding author:** Alessandro Pini, PhD

18 Dipartimento di Medicina Sperimentale e Clinica Sezione di Anatomia e

19 Istologia Università degli Studi di Firenze,

20 Viale Pieraccini 6, 50139, Florence, Italy

21 Phone: +390552758155

22 e-mail: alessandro.pini@unifi.it

23 [1] Present affiliation: Integrated Cardio Metabolic Centre, Department of Medicine, Huddinge

24 (MedH), H7, Karolinska Institute, SE-171 77 Stockholm, Sweden

Abstract

Histamine has been reported to decrease the ultrafiltration coefficient, which inversely correlates with glomerular permselectivity, however the mechanism(s) underling this effect have never been investigated. This study aimed to assess whether histamine could exert a direct detrimental effect on podocyte permeability and the possible involvement of two key proteins for the glomerular slit diaphragm (SD) integrity, zonula occludens-1 (ZO-1) and P-cadherin.

The effect of histamine (100 pM-1000 nM) on coloured podocytes junctional integrity was evaluated functionally by a transwell assay of monolayer permeability and morphologically by electron microscopy. Histamine receptor ($H_{1-4}R$) presence was evaluated at both mRNA (RT-PCR) and protein (immunofluorescence) levels. The K_d and B_{max} values for [^{3}H]mepyramine were detemined by saturation binding analysis; IP_1 and cAMP production evoked by histamine were measured by TR-FRET. ZO-1, P-cadherin and vimentin expression was assessed by qRT-PCR and quantitative immunoblotting.

Histamine elicited a time- and sigmoidal dose-dependent (maximum effect at 8 h, 10 nM) increase in podocyte paracellular permeability widening the paracellular spaces. Only H_1R was predominantly localised to the podocyte membrane. Consistently, histamine elicited a sigmoidal dose-dependent increase in IP_1, but not in cAMP. Histamine exposure evoked a concentration-dependent reduction in both ZO-1 and P-cadherin and a parallel induction of vimentin mRNA expression with a maximum effect after 6 h, and protein expression with a maximum effect after 8h. These effects were prevented by the selective H_1R antagonist chlorpheniramine.

In conclusion, our data demonstrate that histamine, via the H_1R, modifies SD morphological and functional integrity, in part, by decreasing the expression of ZO-1 and P-cadherin.

Keywords: histamine, podocytes, paracellular permeability, histamine receptors, junction integrity.

2

49 **Abbreviations** cAMP, cyclic adenosine monophosphate; *CDH3*, cadherin 3, type 1, P-cadherin

50 gene; ER, endoplasmic reticulum; FITC, fluorescein; *GADPH*, glyceraldehyde 3-phosphate

51 dehydrogenase gene; GBM, glomerular basement membrane; $H_{1-4}R$, histamine receptor $_{1-4}$ subtypes;

52 K_f, ultrafiltration coefficient; IP_1, inositol monophosphate; IP_3, inositol 1,4,5-trisphosphate; PAN,

53 puromycin aminonucleoside; qRT-PCR, quantitative real-time PCR; SD, slit diaphragm; TBP,

54 TATA-binding protein; *TJP1*, tight junction protein 1 gene; TR-FRET, Time-Resolved

55 Fluorescence Resonance Energy Transfer; *VIM* vimentin gene; ZO, Zonula Occludens

56

1 Introduction

58 Histamine is a pleiotropic vasoactive amine, whose pathogenic role in microvascular endothelial

59 paracellular permeability has been extensively studied [1-7]. Most of these studies describe acute

60 events (within seconds to minutes), resulting in a rapid transient increase in permeability, due to a

61 rapid formation of endothelial gaps [2-7]. Moreover, histamine has been suggested to be involved in

62 prolonged vascular leakage by reducing Zonula Occludens (ZO)-1 protein expression in cultured

63 retinal microvascular endothelial cells within hours [8]. The work by Takeuchi K and colleagues

64 (2001) suggested that histamine-induced paracellular permeability might be also extended to other

65 epithelial cells. In particular, histamine was shown to significantly downregulate ZO-1 mRNA

66 expression in cultured human nasal epithelial cells [9]. ZO-1 contributes to the functional integrity

67 of different permeability barriers among which the glomerular filter is one [10]. Interestingly,

68 histamine has been previously reported to decrease the ultrafiltration coefficient (K_f) [11]. Thus, our

69 hypothesis was that histamine could modify K_f by regulating ZO-1 expression in the podocyte.

70 Podocytes are parenchymal cells known to be highly dynamic and terminally differentiated. They

71 interact with the glomerular basement membrane (GBM) and communicate through various

72 signalling pathways at the slit diaphragm (SD). The glomerular SD represents the junction structure

73 that links the interdigitating foot processes from neighbouring podocytes and consists of

74 transmembrane-bridging proteins networking with a juxtaposed cytoplasmic platform of protein

complexes, which in turn is linked to the actin cytoskeleton [12]. Within this cytoarchitecture, ZO-1 protein is located at the cytoplasmic face of the SD [13] and has been accepted to be one of its functional molecules; a disrupted interaction and distribution of ZO-1 in podocytes results in loss of SD structure and function [14-16]. Besides the transmembrane protein, P-cadherin, a podocyte specific adhesion protein [17] localised on adherens-type junctions, mediates calcium-dependent cell-cell bonds and its loss is recognised as a cause of barrier filtration integrity impairment [18]. Therefore, it is likely that glomerular injury affecting ZO-1 and/or P-cadherin results in loss of SD structure, podocyte detachment, K_f reduction and in a subsequent impairment of the filtration barrier integrity with proteinuria, progressive renal damage and eventual loss of renal function [12, 19, 20].

Among the histamine receptor subtypes, $H_{1-4}R$, H_1R and H_2R were first described in mammalian glomeruli [21-23], but these studies were focused on the entire glomerulus or only on stromal cells such as mesangial cells; little is known about parenchymal cells. Indeed, the data on histamine receptors expression on renal parenchymal cells arise only from our recent observations of H_1R, H_2R, H_3R and H_4R on tubular epithelial cells [24-26]. However, no such studies have to date focused on podocytes.

Thus, the present study was designed to investigate whether histamine could exert a direct detrimental effect on podocyte permeability compromising SD functional integrity, the underlying histamine receptor pharmacology, and the possible involvement of two key SD-associated proteins ZO-1 and P-cadherin.

2 Materials and Methods

2.1 Materials

All reagents and chemicals used were from Sigma–Aldrich (St. Louis, MO) unless otherwise noted. Cell media and reagents were from Lonza group Ltd. (Allendale, NJ, USA). Hans Balanced Salt Solution was from GIBCO (Grand Island, NY). HTS Transwell inserts were from Corning Life

Sciences (Lowell, MA). RevertAid™ First Strand cDNA Synthesis Kit, GeneRuler™ 50 bp DNA Ladder, DNA Gel Loading Dye (6X), CellMask™ Orange plasma membrane stain, MagicMark™ XP Western Protein Standard and Alexa-Conjugated secondary antibodies donkey anti-Mouse IgG (A-31570), chicken anti-Goat IgG (A-21469) and goat anti-Rabbit IgG (A-11034) were from Thermo Fisher Scientific Inc. (Rockford, IL, USA). EuroTaq DNA polymerase as well as EuroGOLD Trifast™ were from Euro-clone (Milan, Italy). High Capacity cDNA Reverse Transcription Kit and Power SYBR Green PCR Master Mix were from Applied Biosystems (Foster City, CA). Sequence-specific oligonucleotide primers were purchase from Sigma-Genosys (Milan Italy). The antibodies for histamine H_1R (H300, sc-20633), H_2R (A20, sc-33973), calnexin (AF18, sc-23954), ZO-1 (C-19, sc-8146), P-cadherin (H-105, sc-7893), vimentin (C20, sc-7557) and UltraCruz™ Autoradiography Film were purchased from Santa Cruz Biotechnology Inc. (Dallas, TX, USA), while anti-rabbit and anti-mouse IgG HRP-linked antibodies were from Cell Signaling Technology, Inc. (Danvers, MA, USA) and the swine anti-Goat IgG antibody from Cedarlane Labs (Ontario, Canada). The LANCE® Ultra cAMP Detection Kit, the IP-One HTRF® assay kit, the [^{3}H]mepyramine [PubChemCID 656400; kindly provided by Prof. Rob Leurs (20 Ci/mmol) VU University Amsterdam, Amsterdam] and the Whatman™GF/C Glass Fiber Filter Paper were from PerkinElmer Inc. (Waltham, MA, USA) and Cisbio Bioassays (France), respectively. Precision Plus Protein™ Dual Color Standards and BCA protein assay were from Pierce Bio-technology Inc. (Rockford, IL, USA) and PVDF membrane from Millipore (Bradford, MA, USA). Visiglo™ HRP chemiluminescent substrate kit was purchased from Amresco llc. (Solon, OH, USA).

Histamine dihydrochloride (PubChem CID 5818), (+/-) chlorpheniramine maleate (PubChem CID 5281068), [^{3}H]mepyramine and difenhydramine (Pubmed CID 3100) were dissolved in dimethyl sulfoxide, and the final drug concentrations were obtained by dilution of stock solutions in the experimental buffers. The final concentration of the organic solvent was less than 0.1%, which had no effect on cell viability.

2.2 Cell cultures

126 Immortalised human podocytes were obtained from the respective primary cells, derived from the

127 normal portion of cortex surgically removed kidneys (n=5) for as described previously [27], by

128 infection with a hybrid Adeno5/SV40 virus as previously described [27-29]. The line was generated

129 in 1997, after the authorization of the local Ethical Committee (Hospital San Giovanni Battista

130 "Molinette", Turin, Italy). Podocytes were isolated from the healthy tissue derived from kidney

131 samples of patients who underwent unilateral nephrectomy due to local renal carcinomas as first-

132 line treatment. To our knowledge, no other relevant pathology was diagnosed in the medical history

133 of each patient enrolled and the derived podocytes can be reasonable assumed as healthy podocytes.

134 Podocytes were characterised for the positive expression of nephrin, podocin, and synaptopodin and

135 for negative expression of von Willebrand factor, CD31, and smooth muscle cell actin. Cells were

136 cultured in DMEM containing 4.5 mg/l glucose supplemented with 10% Fetal Calf Serum,

137 penicillin/streptomycin (100 IU/ml), and l-glutamine and the cultures were maintained at 37 °C in a

138 95% air/5% CO_2 humidified incubator.

139 **2.3 Permeability assay**

140 Podocyte monolayer permeability was determined as previously described [30, 31]. Human

141 immortalised podocytes (40,000 cells well, 500 μl) were seeded on the top of HTS Transwell inserts

142 (3 μm pore, 24-well plate) and cultured till confluence was achieved. Cells were washed twice with

143 PBS supplemented with 1 mM $MgCl_2$ and 1 mM $CaCl_2$ and then pre-treated with vehicle alone or

144 chlorpheniramine maleate 10 μM for 10 min before exposure to histamine 0.01-1000 nM for 0-8 h.

145 Fluorescein (FITC)-labeled bovine serum albumin was added to the bottom chambers of the

146 transwells and medium fluorescence activity in the top chambers was measured at selected time-

147 points with a fluorescence plate reader (excitation: 495 nm, emission: 520 nm; multiple plate reader

148 Victor X4; PerkinElmer Inc.). Fold-change in expression with respect to the control mean was

149 calculated for all samples.

150 **2.4 Electron microscopy**

151 Podocytes pre-treated with vehicle alone or chlorpheniramine maleate 10 μM for 10 min before

152 exposure to histamine 10 nM or 0.1 nM for 0-8 h were fixed in 4% glutaraldehyde and post-fixed,

153 after pelleting, in 1% osmium tetroxide and embedded in Epon 812. Ultrathin sections were stained

154 with uranyl acetate and alkaline bismuth subnitrate and examined under a JEM 1010 electron

155 microscope (Jeol, Tokyo, Japan) at 20 kV and 50 kV. Morphometrical analysis were performed on

156 50KV digitized images using ImageJ 1.41 software (http://rsbweb.nih.gov/ij; NIH, USA) in 20

157 regions of interest (ROI) for each sample.

158 *2.5 RT-PCR*

159 Two μg/μl of total RNA extracted from podocytes by using RevertAid™ First Strand cDNA

160 Synthesis Kit according to the manufacturer's instruction, were subjected to RT-PCR as previously

161 described [26, 32]. The subsequent specific oligonucleotide sequences were used: *hH1R* forward 5'

162 CATTCTGGGGGCCTGGTTTCTCT-3' and reverse 5'-CTTGGGGGTTTGGGATGGTGACT-3';

163 *hH2R* forward 5'-CCCGGCTCCGCAACCTGA-3' and reverse 5'-

164 CTGATCCCGGGCGACCTTGA-3'; *hH3R* forward 5'-CTTCCTGCCCTAGCAGTT-3' and reverse

165 5'-GCAGAGAACAGCTTCGAGGTT-3' *hH4R* forward 5'-TGGAAGCGTGATCATCTCAG-3'

166 and reverse 5'-ATATGGAGCCCAGCAAACAG-3'. PCR amplicons were resolved in an ethidium

167 bromide-stained agarose gel (2.5%) by electrophoresis. GAPDH gene expression was used as an

168 internal control.

169 *2.6 Immunocytofluorescence and confocal analysis*

170 Podocytes plated on collagen-coated cover glasses were fixed with 4% paraformaldehyde for 10

171 minutes at room temperature. H_4R was detected using The anti-hH_4R (374–390) antibody produced

172 and validated for detecting both human and rodent H_4R in the School of Biological and Biomedical

173 Sciences, Durham University [33-39]. Sections were incubated overnight with anti-H_1R (1.3

174 μg/ml), anti-H_2R (1.3 μg/ml) or anti-H_4R (2 μg/ml) receptor subunit at 4°C. Subsequently, for

175 endoplasmic reticulum (ER) cells were incubated with anti-calnexin (2 μg/ml) followed by

incubation with the respective Alexa-Conjugated secondary antibodies. The negative control to exclude non-specific staining by the secondary antibody (where cells were incubated with secondary antibodies alone) is reported in Supplementary Material Fig. 1. The plasma membrane was stained using CellMask™ Orange plasma membrane stain according to the manufacturer's protocol. Cells were fixed with 4% paraformaldehyde and processed for histamine receptors staining. Nuclei were stained with Hoescht.All the slides were examined at ×63 magnification using the SP5 Confocal Laser Scanning Microscope SMD (Leica). A variable number of optical section images in the z-dimension (z-spacing, 0.42μm) were collected ensuring that images throughout the 3D cellular structure, spanning multiple confocal planes, were fully captured. Maximum projection of the confocal images were analyzed quantitatively for the extent of colocalization of $H_{1-4}Rs$ with each of the sub-compartment marker proteins using the ImageJ software package.

2.7 Radioligand binding studies

The saturation binding isotherms were determined by incubating washed podocyte homogenates for 45 min at 25°C with 0–16 nM $[^3H]$ mepyramine and assay buffer (50 mM phosphate buffer pH 7.4) in a total assay volume of 200 μl.The incubation was stopped by rapid dilution with ice-cold assay buffer. Non-specific binding was determine using unlabelled 10 μM difenhydramine. The bound radioactivity was separated by filtration through GF/B Glass Fiber Filter Paper that had been treated with 0.3% polyethyleneimine (PEI). Filters were washed thrice with ice-cold assay buffer and the radioactivity retained on the filters was measured by liquid scintillation counting. Protein concentrations were determined according to Bradford methods, using bovine serum albumin as a standard.

2.8 Time-Resolved Fluorescence Resonance Energy Transfer (TR-FRET)

The TR-FRET assay was used to evaluate both cAMP and IP_1 production by using the LANCE® Ultra cAMP Detection Kit and the IP-One HTRF® assay kit, respectively, as previously described [26] and according to their manufacturer's instruction. The energy transfer was measured by the multiple plate reader Victor X4 (excitation: 620 nm, emission: 665 nm).

202   *2.9 Quantitative real-time PCR (qRT-PCR)*

203   qRT-PCR was performed on RNA isolated by EuroGOLD Trifast™ according to the

204   manufacturers' instructions from podocytes (80% confluence) pretreated with vehicle alone or with

205   chlorpheniramine maleate at 10 μM and challenged with histamine in the range 3 pM-1000 nM for

206   0-8 and 24 h. Briefly, first-strand cDNA was produced from 200 ng of total RNA using the High

207   Capacity cDNA Reverse Transcription Kit. Real-time PCR experiments were performed in 20-μl

208   reaction mixture containing 5 ng of cDNA template, the sequence-specific oligonucleotide primers

209   (*TJP1* forward: CATCAGATCATTCTGGTCGATCA and reverse: TCCGGAGACTGCCATTGC;

210   *CDH3*   forward: CCAGCTTGGGCAACATAGGGTand   reverse:

211   TCAGCTCCCGCTGAGACTACA; *VIM* forward: GGAACAGCATGTCCAAATCGATand

212   reverse: CAGCAAACTTGGATTTGTACCATT), and the Power SYBR Green PCR Master Mix.

213   TATA-binding protein (TBP) mRNA were used to normalise RNA inputs. The relative expression

214   of mRNA was calculated according to the $2^{(-\Delta Ct)}$ method. Fold-change expression with respect to

215   control was calculated for all samples.

216   *2.10 Immunoblotting*

217   Sixty μg of proteins, extracted by EuroGOLD Trifast™ according to the manufacturers'

218   instructions from podocytes (80% confluence) exposed to vehicle alone or pretreated with vehicle

219   alone or with chlorpheniramine maleate and challenged with histamine in the range 3 pM-1000 nM

220   for 0-8 and 24 h, were subjected to SDS-PAGE using a 8 % gel. The PVDF membrane was blotted

221   over-night with goat polyclonal anti-ZO-1, rabbit polyclonal anti-P-cadherin or goat polyclonal

222   anti-vimentin antibodies (1 μg/ml in PBS) and then re-probed with mouse monoclonal anti-β-actin

223   antibody (1:5000) to confirm the homogeneity of the proteins loaded. The membranes were

224   overlaid with Visiglo™ HRP chemiluminescent substrate kit and then exposed to Hyperfilm ECL

225   film. Densitometric analysis was performed by ImageJ software package. Fold-change expression

226   with respect to control was calculated for all samples.

227   *2.11 Data analysis and statistical procedures*

228 Gene and protein expression data are expressed as fold-changes relative to the control (vehicle

229 alone), which is represented as one-fold. For the permeability assay the mean of the control values

230 have been calculated and all the individual control values and all the individual test values are

231 expressed as fold-change relative to the control mean. Results are shown as mean ± SEM from 5

232 different experiments, and were analysed by Prism 4 software from Graphpad (CA, USA). The test

233 for normality using the Kolmogorov-Smirnov followed by the one-way ANOVA and the *post-hoc*

234 Dunnett's multiple comparison were performed when there was a variance homogeneity

235 (permeability assay). In all the other cases, the non-parametric Kruskal-Wallis test was used. For

236 concentration-response curves a four-parameter logistic equation was applied and the best-fit was

237 obtained. Radioligand binding data were evaluated by a nonlinear, least-squares curve-fitting

238 procedure using GraphPad Prism 5. To determine significant differences between means, the

239 threshold for statistical significance was set to P-values < 0.05.

240 **3 Results**

241 ***3.1 Histamine compromises SD integrity in human immortalised podocytes***

242 We tested whether the amine influences the transepithelial flow of FITC-albumin in a transwell

243 assay of monolayer permeability. We found that histamine treatment (0.01-10 nM; 0-8 h) time- and

244 concentration-dependently and significantly increased fluorescence intenstity in the top chamber

245 beginning from 6 h (basal level of Fluorescence intensity = 15651 ± 950 FU; $P< 0.05$) up to 160%

246 at 8 h ($P<0.01$; Fig. 1a) with an EC_{50} of about 0.1 nM (Fig. 1b). Notably, the 10 min pre-treatment

247 of podocytes with chlorpheniramine maleate was effective in preventing the transepithelial flow of

248 FITC-albumin, as demonstrated by its ability to partially prevent the effect exerted by histamine 0.1

249 nM (Fig. 1c).
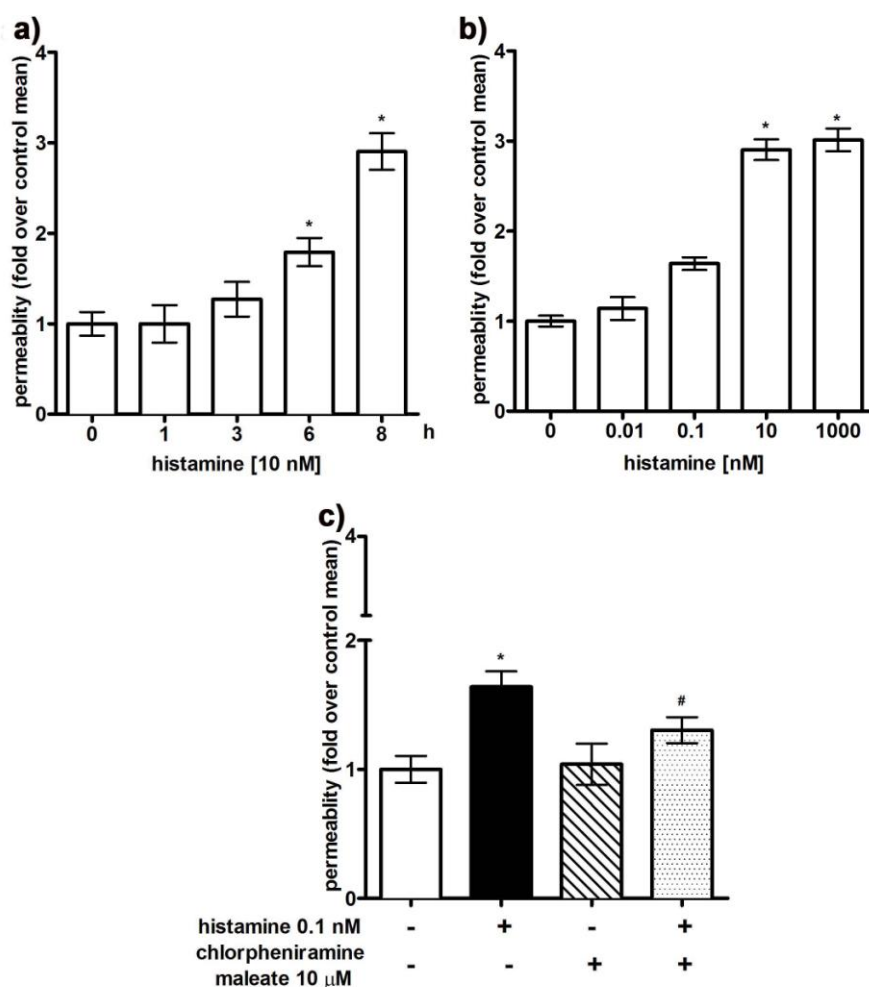
Fig. 1. Junction functional integrity of human immortalized podocyte. Transepithelial albumin permeability of podocyte monolayer was measured using FITC-BSA. (**a**) Cells were exposed to histamine 10 nM from 0 to 8 h. Data, expressed as fold-change over control mean, are means ± SEM of 5 independent experiments. Statistical analysis was performed by one-way ANOVA and Dunnett test. *$P< 0.05$ *versus* time 0. (**b**) Cells were exposed to histamine 0 - 1000 nM for 8 h. Data, expressed as fold-change over control mean, are means ± SEM of four independent experiments. Statistical analysis was performed by one-way ANOVA and Dunnett test. *$P< 0.05$ *versus* concentration 0. (**c**) Podocytes pretreated for 10 min with vehicle alone or the selective H_1R antagonist, chlorpheniramine maleate 10 μM, were exposed to histamine (0.1 nM) for 8 h. Data, expressed as fold over control, are means ± S.E.M. of 5 independent experiments. *$P< 0.05$ *versus* vehicle alone and [#]$P< 0.05$ *versus* histamine 0.1 nM.

263   The detrimental effect of H_1R activation on SD was strongly validated when the junction integrity

264   was quantitatively evaluated by electron microscopy. The width of the intercellular space was

265   narrow and constant throughout the contact area in the control cells (Fig. 2a and b) whereas it was

266   significantly compromised after histamine exposure for 8 h at 0.1 nM (Fig. 2b), appearing to be

267   discontinuous and uneven with widening of the paracellular spaces after histamine exposure for 8 h

268   at 0.1 nM. The pre-treatment with chlorpheniramine maleate was able to ameliorate the histamine

269   evoked-effects as intercellular spaces appeared narrower, although this was incomplete (Fig. 2a and

270   b). Chlorphenamine treatment alone did not affect the intercellular contact area.
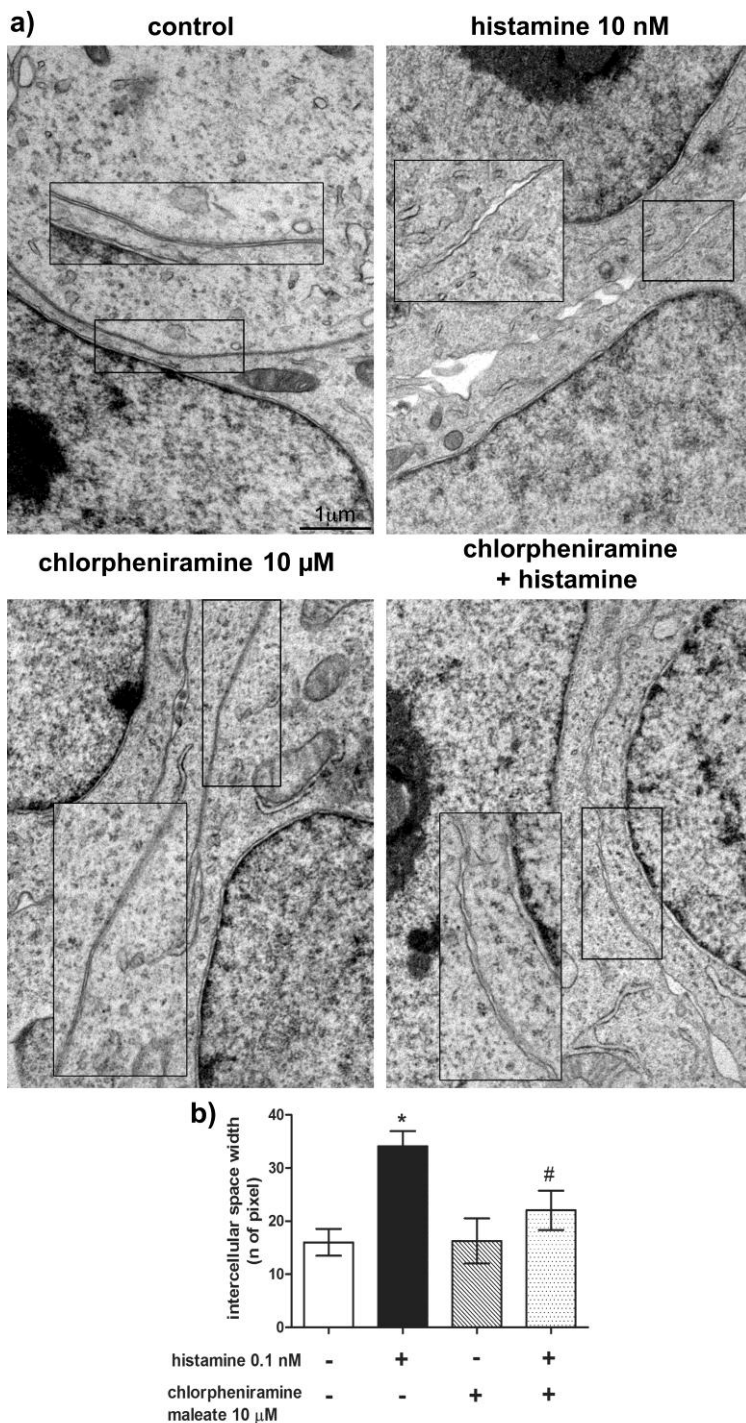
Fig. 2 Chlorpheniramine effect on junction integrity. (**a**) Representative images of ultrathin sections from human immortalized podocytes pretreated for 10 min with vehicle alone or the selective H_1R antagonist, chlorpheniramine maleate 10 μM, were exposed to histamine (0.1 nM) for 8 h. The morphological assessment of the junction integrity was carried out in three different experiments. Sections were examined under a JEM 1010 electron microscope at 20 kV. The insets show the integrity junctional level detail evaluated at 50 kV. (**b**) Quantitative analysis of the

278   intercellular junction morphology performed on 50KV digitized images. Data, expressed as fold-

279   change over control, are means ± S.E.M. for n = 20 regions of interest (ROI) for each sample. *$P<$

280   0.05 *versus*   vehicle alone and #$P<$ 0.05 *versus* histamine 0.1 nM.

281

282   **3.2 Histamine receptor expression in human immortalised podocytes**

283   In order to further explore the underlying histamine pharmacology, the expression of histamine

284   receptors in human immortalised podocytes was evaluated at both the gene and protein levels.

285   Moreover, their functional expression was confirmed by TR-FRET assay evaluating the second

286   messenger production induced by histamine. As shown in Fig. 3a, RT-PCR analysis revealed single

287   transcripts corresponding to the predicted size for *H1R* (403 bp) and *H4R* (353 bp); *H2R* (497 bp)

288   was at the limit of detection. No transcript for *H3R* (221 bp) was detected. Consistent results were

289   obtained when protein expression was evaluated by immunocytofluorescence and confocal analysis

290   (Fig. 3b and c). Indeed, H_1R showed a robust staining with a prominent membrane localisation as

291   demonstrated by its colocalisation with CellMask™ plasma membrane stain (Pearson's coefficient,

292   r = 0.62; Mander's coefficients threshold for channel 1, red staining, tM1 = 0.38 and Mander's

293   coefficients threshold for channel 2, green staining, tM2 =0.93); moreover, H_1R coimmunolabelling

294   with calnexin (r = 0.59; tM1 = 0.76 and tM2 = 0.59), suggestive of the presence of a proportion of

295   H_1R on the ER, was also revealed. In comparison, H_4R immunolabeling showed a lower

296   immunopositivity level, predominantly within the cytoplasm where a partial positivity was found in

297   the ER (r = 0.21, tM1 = 0.30 and tM1 = 0.22 for the colocalization within the membrane and r =

298   0.29, tM1 = 0.28 and tM2 = 0.33 for the colocalization within the ER; Fig.3b and c). Very modest,

299   if any, membrane colocalisation was revealed. The staining for H_2R was at the limit of the detection

300   and was not possible to localise it within the membrane.
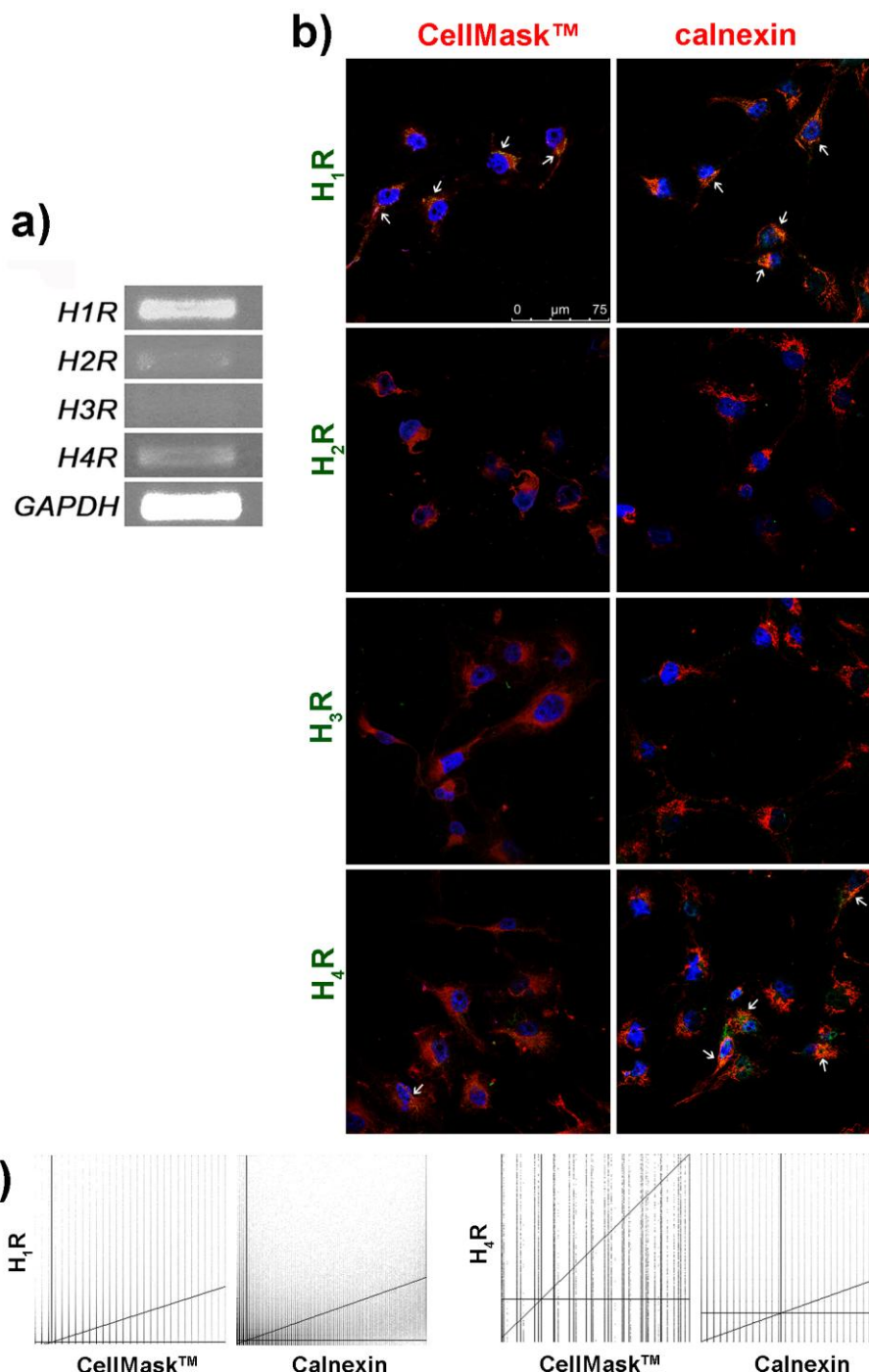
Fig. 3 Histamine receptor expression in human immortalized podocytes. (**a**) Agarose gels representative of 5 independent RT-PCR assays for cDNA from human immortalized podocyte. Single transcripts corresponding to the size predicted for *H1R* (403 bp), *H2R* (497 bp), *H3R* (221 bp), and *H4R* (353 bp) were detected. The housekeeping gene *GAPDH* was used as control. (**b**) Representative merged immunofluorescence images from 5 independent experiments where cells were labelled with specific anti-H_1 anti-H_2, anti-H_3, or anti-H_4 receptor antibodies (green),

308 respectively, calnexin or CellMask™ Plasma Membrane Stains (red). Nuclei were stained with

309 Hoescht (blue). Detection of yellow colouration, shown by arrows, indicates colocalization.All the

310 slides were examined at ×63 magnification using the SP5 Confocal Laser Scanning Microscope

311 SMD (Leica). (**c**) Scatterplot of red and green pixel intensities of the maximum projection of the

312 image volume in (**b**).

313

314 These data suggested the presence of H_1R on the surface of human podocytes, therefore a saturation

315 binding study with the H_1R antagonist mepyramine were performed to quantify the receptor levels.

316 The saturation isotherms revealed a K_d for [^{3}H] mepyramine of 7.02 ± 1.76 nM, indicating the

317 presence of a single class of high affinity binding sites in podocyte membranes. The binding was

318 saturable with a B_{max} estimate of 376 ± 39 fmol/mg protein (Fig. 4a).

319 To further confirm our findings, we tested the activation of the histamine receptors evaluating the

320 levels of cAMP and IP_3 second messengers evoked by histamine. As shown in Fig. 4b, podocytes

321 challenged with histamine (3 pM-10 nM) did not show any changes in cAMP levels, the second

322 messenger predominantly coupled with G_s (such as H_2R) and with G_i (such as H_3R and H_4R)

323 receptors. Notably, cells exposed for 1 h to histamine 3 pM-10 nM showed a concentration-

324 dependent decrease in TR-FRET signal, indicating a sigmoidal increase of IP_1 (EC_{50} 0.15 ± 0.03

325 nM). The pre-treatment for 10 min with the selective H_1R antagonist chlorpheniramine maleate at

326 either 1 µM or 10 µM shifted rightwards in a parallel fashion the curve evoked by histamine in a

327 dose-dependent manner (chlorepheniramine maleate alone did not affecteither cAMP or IP_1

328 production; data not shown). Taken together, these data confirm the functional expression of H_1R

329 on podocyte membrane.
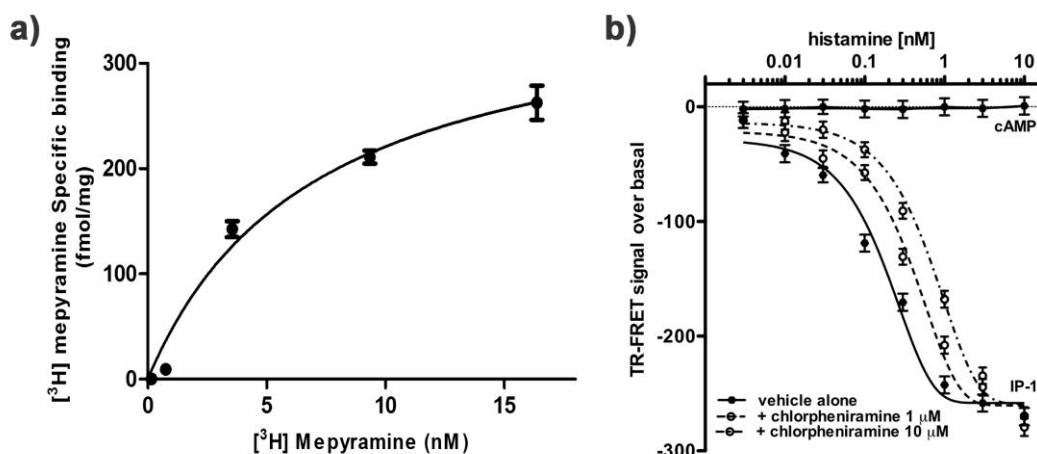
Fig. 4 Histamine receptor pharmacological profile in human immortalized podocytes. Saturation binding curve for [^{3}H]mepyramine binding to podocyte cell membrane homogenates (**a**). Data are the mean ± SD of 3 separate cell preparations determined in triplicate. (**b**) The levels of IP$_1$, downstream metabolite of IP$_3$, and of cAMP were measured, according to the manufacturer's instruction, by IP-One HTRF® assay kit (Cisbio) or by LANCE Ultra cAMP assay (PerkinElmer), respectively. Human immortalized podocytes were pretreated for 10 min with vehicle alone (black hexagon, solid line for IP$_1$ and white square solid line for cAMP) or the selective H$_1$R antagonist, chlorpheniramine maleate 1 μM (white circle, dash line) or 10 μM (white circle, dash-dot line), were exposed to histamine (3 pM – 10 nM). Results, expressed as TR-FRET signal over the basal and represented as best-fit concentration-response curve, are the mean ± SEM of 5 independent experiments run in duplicate.

3.3 Histamine affects SD protein expression in human immortalized podocyte

The effect evoked by histamine on SD associated proteins ZO-1 and P-cadherin was evaluated at both gene and protein levels. As shown in Fig. 5a and Fig. 6a, cells challenged with histamine (1 pM–10 nM up to 8 h) showed a time- and concentration-dependent reduction of both TJP1, the gene encoding for ZO-1, and CDH3, the encoding gene for P-cadherin, with a maximum of approx. 50% after 6 h. Consistently, similar results with a maximum effect at 8 h were obtained when protein expression was evaluated (Fig. 5b and c, and Fig. 6b and c).Moreover, histamine evoked a parallel

17

350 induction of the intermediate filament vimentin expression (Figure 5a, b and c and Figure 6a, b and

351 c), a mesenchymal marker associated with podocyte effacement and detachment [40].

352
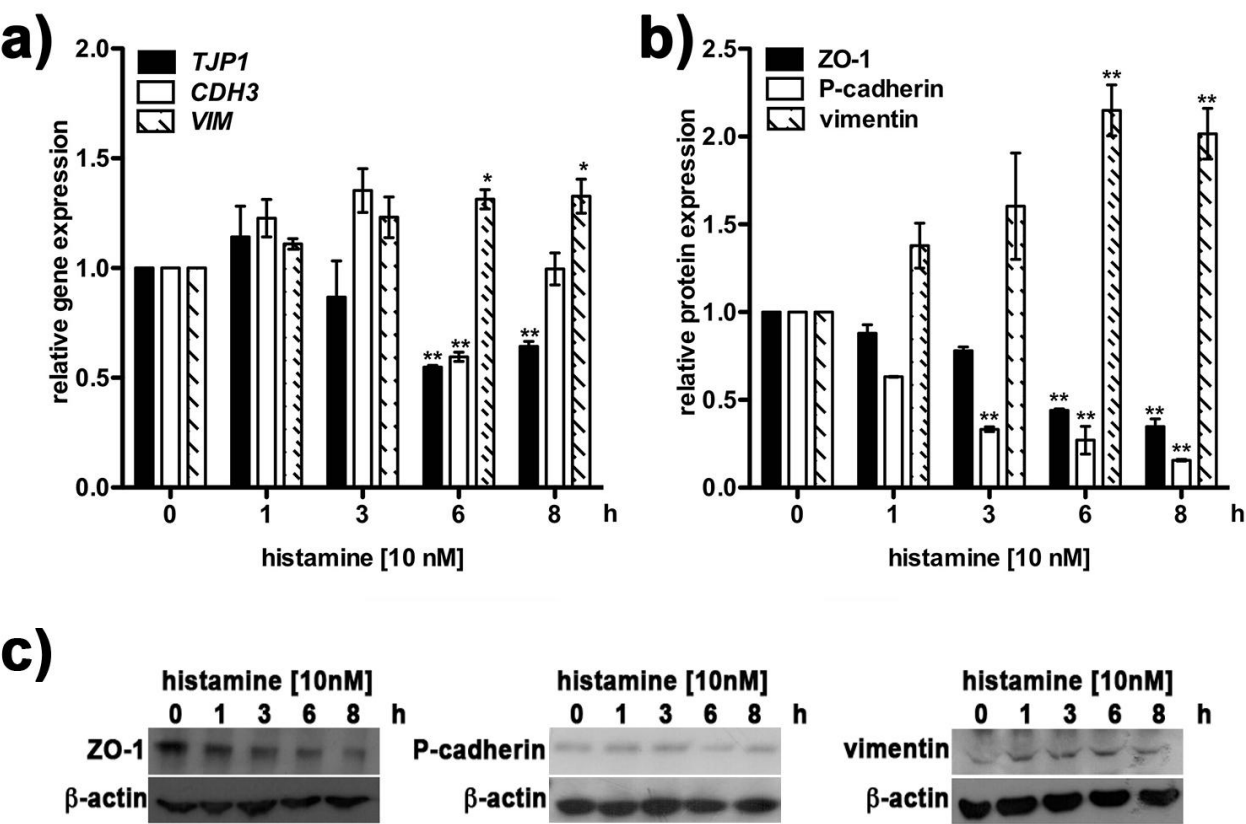
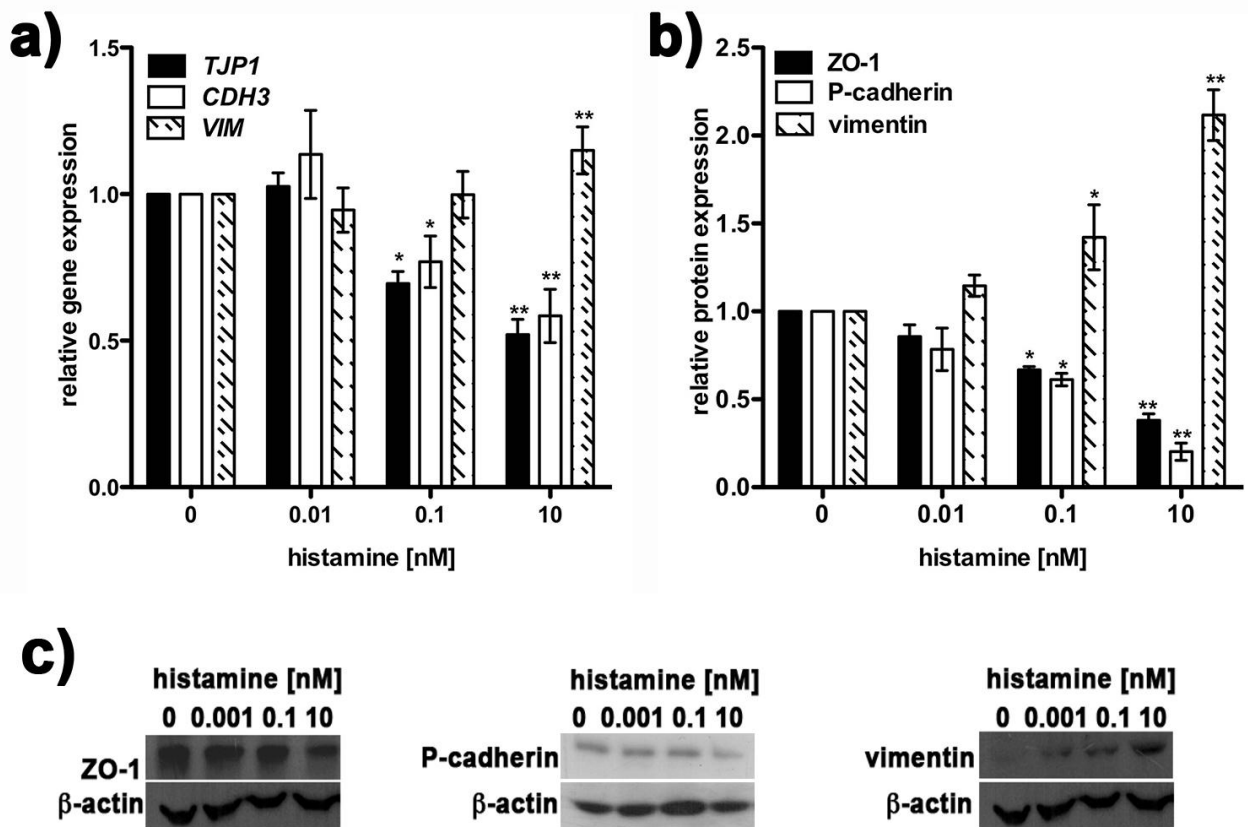353 **Fig. 5 Effect evoked by histamine on ZO-1, P-cadherin and vimentin expression: time-course**.

354 Effect evoked by histamine on ZO-1, P-cadherin and vimentin expression: time-course. Human

355 immortalized podocytes were treated with histamine (10 nM) from 0 to 8 h. At selected time *TJP1*,

356 *CDH3* and *VIM* expression was evaluated by qRT-PCR (**a**) and ZO-1, P-cadherin and vimentin

357 protein expression was determined by Western blot analysis (**b**); results are expressed as mean ±

358 SEM of five independent experiments; *P< 0.05 *versus* time 0. Pictures shown are representative of

359 five independent immunoblotting experiments (**c**).

360

Fig. 6 Effect evoked by histamine on ZO-1, P-cadherin and vimentin expression: concentration-response. Human immortalized podocytes were treated with histamine (0-10 nM) for 6 or 8 h and processed for TJP1, CDH3 and VIM expression by qPCR (**a**) and ZO-1, P-cadherin and vimentin protein expression by Western blot analysis (**b**), respectively; results are expressed as mean ± SEM of five independent experiments, *$P < 0.05$ *versus* 0 (vehicle alone). Pictures shown are representative of five immunoblotting independent experiments (**c**).

Notably, in our experimental condition, synaptopodin and podocin expression, both markers of podocyte differentiation, was not affected (Supplementary Material Fig. 2)

When cells were pre-treated with the selective antagonists chlorpheniramine maleate 10 µM, a parallel rightward shift of the curves evoked by histamine was observed with an increase in EC_{50} from 0.09 ± 0.03 nM to 7.62 ± 1.44 nM for ZO-1 (Fig. 7a), from 0.13 ± 0.25 nM to 8.57 ± 2.25 nM

for P-cadherin (Fig. 7b) and from 2.40 ± 1.23 nM to 9.76 ± 3.23 nM for vimentin (Fig. 7c),

respectively.
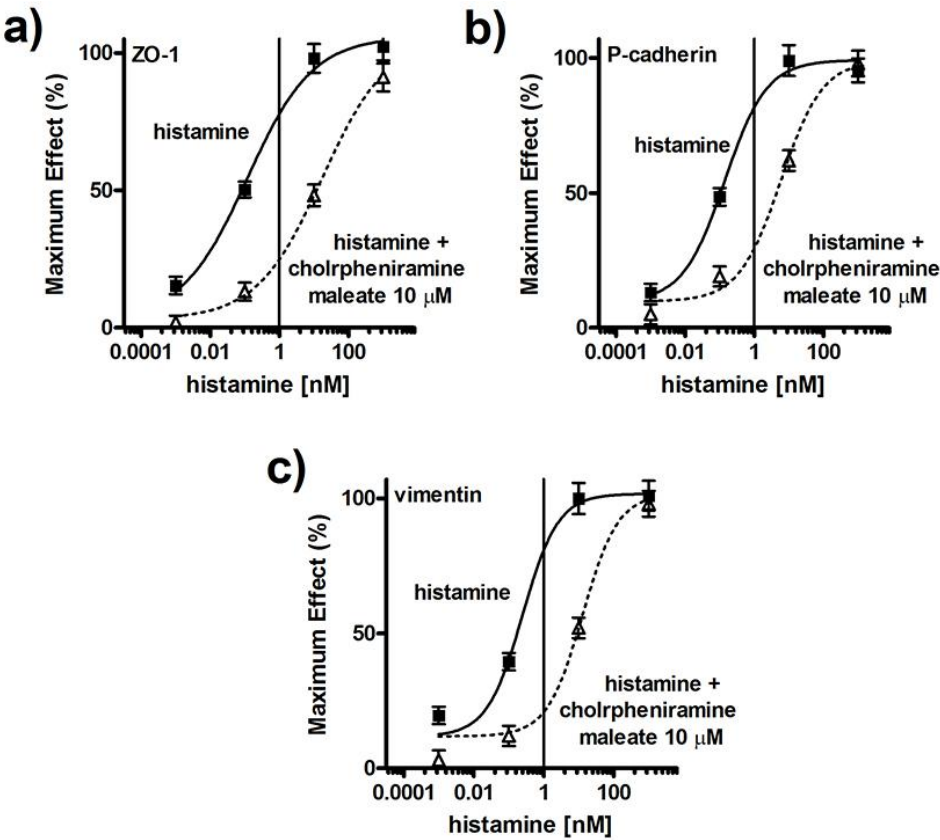
Fig. 7 Chlorpheniramine antagonism on ZO-1, P-cadherin and vimentin expression evoked by histamine. Human immortalized podocytes pretreated for 10 min with vehicle alone or the selective H_1R antagonist, chlorpheniramine maleate 10 μM were treated with histamine for 8 h and processed for ZO-1 (**a**), P-cadherin (**b**) and vimentin (**c**) protein expression. Results, represented as best-fit dose-response curve, are expressed as mean ± SEM of 5 different experiments.

4 Discussion and Conclusions

This study demonstrates for the first time that histamine, via the H_1R, exerts a detrimental direct effect on SD integrity, which results in an increase in podocyte paracellular permeability. This effect is underpinned, in part, by the down-regulation of two key proteins vital for the maintenance of SD integrity, ZO-1 and P-cadherin, with a parallel increase in vimentin expression, the latter probably promoting an epithelial-mesenchymal transition. Interestingly, our study offers, not only a

388 new insight into the effect of histamine on podocyte integrity, but also a clear demonstration of the

389 involvement of histamine in prolonged permeability leakage. Indeed, the extended kinetics of the

390 herein observed events (number of hours) are in keeping and strongly support the delayed

391 mechanism by which histamine increases paracellular permeability involving transcriptional and

392 transductional events [9]. Similar to what was reported for the endothelial junction [41] and in

393 keeping with the ability of histamine to alter adhesion at sites between adjacent cells [42], the

394 results herein suggest that the production of IP_3 by histamine interaction with H_1R triggers the

395 activation of a signalling pathway ultimately resulting in an increase in paracellular permeability.

396 This detrimental effect in the human podocytes is supported by the reduction of the expression of

397 two vital proteins for the SD integrity, ZO-1 and P-cadherin. Notably, although many *in vitro*

398 podocytes cultures showed a cellular dedifferentiation, reflected by loss of processes, and

399 accompanied by a down-regulation of synaptopodyn, our cells displayed a robust mature phenotype

400 as indicated by not only synaptopodin and podocin expression (Supplementary Material Fig. 2a and

401 2c), but also nephrin [43, 44]. Therefore, our *in vitro* system can be considered a suitable new

402 model to study SD-associated proteins. Most notably, our data provide evidence to point to human

403 immortalised podocytes as an interesting new *in vitro* model to study the histaminergic system in

404 naïve human cells. Our *in vitro* cell culture of human immortalised podocytes showed unique

405 expression pattern for both H_1R and HDC enzyme (Supplementary Material Fig. 2a and c), this

406 suggesting that both the autocrine and paracrine effects of this amine could be studied in this

407 system.

408 The unexpected low EC_{50} (ca. 0.1 nM) herein reported for both ZO-1 and P-cadherin, closely

409 comparable to the one evoked by histamine when IP_3 was measured, could be due, in part, to the

410 ability of cells to endogenously produce histamine; indeed, our data show that podocytes clearly

411 express the HDC enzyme (Supplementary Material, Fig. 3 a and b) and that the enzyme is

412 functionally acting, although with a low rate of histamine production (Supplementary Material, Fig.

413 3c). The atypical apparent high potency of histamine, may also reflect changes in local histamine

414 concentrations over time, H_1R membrane expression changes and trafficking during the extended

415 exposure period (1-8h), or a large portion of spare receptors. Moreover, splice variations [45] and

416 polymorphisms [46] in human H_1R have been observed, and their eventually occurrence in our cells

417 cannot be ruled out. Although these alternative forms of H_1R have not been pharmacologically

418 characterized thus far, they could be more sensitive to histamine than the wild-type form. The

419 similar shifts in dose-response curves with the racemic (+/-) chlorpheniramine are consistent with

420 the range of published pA_2 values for native H_1R across species and tissues [47-49].

421 Notably, the similar EC_{50}s for ZO-1, P-cadherin and IP_3 led also to speculate that H_1R activation in

422 human podocytes could initiate different and parallel signaling pathways, which converge in the SD

423 dysregulation. For instance, it has been reported that the elevation in IP_3 triggers the protein kinase

424 C activation and evokes calcium efflux from the ER thus promoting signals to the cytoskeleton,

425 ultimately resulting in the increase in permeability [8, 50-52]. However, histamine could affect the

426 cytoskeleton rearrangement through also a phospholipase C-independent mechanism, evoking the

427 phosphorylated myosin light chains accumulation through the RhoA/Rho-associated coiled kinase

428 pathway and activating the mitogen-activated protein kinase p38 [41, 53]. These warrant further

429 investigation.

430 Radioligand binding studies demonstrate high affinity [^{3}H]mepyamine binding sites in the podocyte

431 cells with a mean K_d value comparable to previously published studies for the human H_1R [54].

432 Consistent with functional data indicating that histamine activates only the canonical H_1R-mediated

433 response (second messenger IP_3, evaluated by IP_1), and not H_2R-, H_3R- or H_4R-mediated response

434 (second messenger cAMP), we found that H_1R is predominantly localised on the plasma membrane.

435 Its partial intracellular presence, suggested by co-localization with calnexin, could reflect the

436 receptor trafficking in the presence of nM histamine concentrations.

437 Actually, in human podocytes, we clearly detected the H_4R receptor at both the gene and protein

438 level, although no functional evidence of H_4R were observed. These data raises the discussion of

439 the selectivity of H_4R antibody [55, 56], however we obtained the same results using different

22

440   commercial H_4R antibodies (Supplementary Material, Fig. 4), at least one of which was validated

441   by $H_4R^{-/-}$ mice. The low level of localisation of the H_4R at the cell membrane could be a possible

442   explanation for the lack of the functional evidence. Indeed, we found a predominantly intracellular

443   localisation accounting for a possible receptor trafficking or for the presence of splice variants of

444   the H_4R. Indeed, the predominant intracellular localisation of H_4R splice variants was already

445   reported by van Rijn and colleagues (2008). However, this speculation needs to be further

446   investigated and also we could not completely rule out the hypothesis that in this cell type, H_4R

447   might activate alternative second messengers, such as the recruitment of ß-arrestin [57].

448   Consistent with our results pointing to H_1R as the only histamine receptor functionally expressed in

449   the podocyte membrane, only the pre-treatment with the competitive H_1R antagonist,

450   chlorpheniramine maleate, shifted the curve to the right, while JNJ7777120, a well-known H_4R

451   antagonist prototype, as well as ranitidine, a well-known anti-H_2 antihistamine drug, were both

452   ineffective (Supplementary Material, Fig. 5). All these molecular events, the activation of H_1R

453   leading to the increase in IP_3 production and the co-incident reduction in ZO-1 and P-cadherin, may

454   represent the possible mechanism underlining the detrimental effect of histamine on junction

455   morphological and functional integrity as suggested by the comparable time- and concentration-

456   response profiles. Notably, although P-cadherin protein expression was already affected after 3 h of

457   histamine challenge, the permeability leakage was evident only after 6 h, when also ZO-1

458   expression was reduced. This evidence is in keeping with previous studies showing that modulating

459   P-cadherin alone is not sufficient for the SD dysregulation [58].

460   In addition to ZO-1 and P-cadherin down-regulation a parallel increase of vimentin expression was

461   also observed. Again the concentration-response profile of vimentin induction by histamine was

462   closely comparable to the one evoked by histamine when IP_3 was measured and, again, only the

463   pre-treatment with chlorpheniramine maleate shifted the curve to the right, thus indicating a pure

464   H_1R-mediated event. The increase of mesenchymal markers, such as vimentin, has been associated

465   with podocyte effacement, detachment and loss in diabetic nephropathy [40]. Indeed, podocyte

dedifferentiation and mesenchymal transition could be a potential pathway leading to their dysfunction, thereby playing a role in the genesis of proteinuria [59].

Histamine was previously demonstrated to alter the link between adherent junction and vimentin in primary human umbilical vein endothelial cells [50]. Moreover, vimentin was also already reported to be upregulated by histamine in primary mouse brain organotypic (MBO) cultures [60]. Vimentin has been also found to be upregulated in podocytes in puromycin aminonucleoside nephrosis [61], a model characterized by the presence of high levels of histamine in the renal cortex, whose abnormal metabolism was postulated to be related both as a cause or a consequence of the pathogenenesis [21].

Interestingly, until now histamine was assumed only to affect the K_f through the H_1R and H_2R present on mesangial cells, in keeping with the theory that contraction of these cells leads to a reduction in the glomerular capillary surface area. We provide for the first time, molecular pharmacological evidence for a direct effect of histamine on human podocytes, suggestive of a possible use of antihistamines as add-on therapy to counteract the onset and progression of both albuminuria and glomeruosclerosis in different renal aetiologies. Previously, this hypothesis was dismissed by the report that histamine and diphenhydramine had no effect on the alterations in glomerular ultrafiltration that occurs shortly after administration of anti-glomerular basement membrane antibody [62] in a model of acute glomerular immune injury in the rat. However, the authors claimed that it was unlikely that later events would differ greatly regarding a role for histamine because of the effects of locally injected histamine are immediate and should be evident early. In our study, we clearly demonstrate that exposure to low concentrations of histamine promotes important later events on the SD and that these could be prevented by chlorpheniramine.

Taken together these data are suggestive of a combined pathophysiological mechanism of histamine on K_f, it evokes not only the mesangial cell contraction but also may promote delayed podocyte detachment, the loss of SD integrity, and subsequent proteinuria and eventual renal damage.

Conflicts of Interest

None

References

[1] G. Majno, S.M. Shea, M. Leventhal, Endothelial contraction induced by histamine-type mediators: an electron microscopic study, The Journal of cell biology 42(3) (1969) 647-72.

515   [2] J.J. Killackey, M.G. Johnston, H.Z. Movat, Increased permeability of microcarrier-cultured

516   endothelial monolayers in response to histamine and thrombin. A model for the in vitro study of

517   increased vasopermeability, The American journal of pathology 122(1) (1986) 50-61.

518   [3] D. Rotrosen, J.I. Gallin, Histamine type I receptor occupancy increases endothelial cytosolic

519   calcium, reduces F-actin, and promotes albumin diffusion across cultured endothelial monolayers,

520   The Journal of cell biology 103(6 Pt 1) (1986) 2379-87.

521   [4] K.K. Hamilton, P.J. Sims, Changes in cytosolic Ca2+ associated with von Willebrand factor

522   release in human endothelial cells exposed to histamine. Study of microcarrier cell monolayers

523   using the fluorescent probe indo-1, The Journal of clinical investigation 79(2) (1987) 600-8.

524   [5] T.A. Brock, E.A. Capasso, Thrombin and histamine activate phospholipase C in human

525   endothelial cells via a phorbol ester-sensitive pathway, Journal of cellular physiology 136(1) (1988)

526   54-62.

527   [6] M.R. Carson, S.S. Shasby, D.M. Shasby, Histamine and inositol phosphate accumulation in

528   endothelium: cAMP and a G protein, The American journal of physiology 257(4 Pt 1) (1989) L259-

529   64.

530   [7] N. Niimi, N. Noso, S. Yamamoto, The effect of histamine on cultured endothelial cells. A study

531   of the mechanism of increased vascular permeability, European journal of pharmacology 221(2-3)

532   (1992) 325-31.

533   [8] T.W. Gardner, T. Lesher, S. Khin, C. Vu, A.J. Barber, W.A. Brennan, Jr., Histamine reduces

534   ZO-1 tight-junction protein expression in cultured retinal microvascular endothelial cells, The

535   Biochemical journal 320 (Pt 3) (1996) 717-21.

536   [9] K. Takeuchi, C. Kishioka, H. Ishinaga, Y. Sakakura, Y. Majima, Histamine alters gene

537   expression in cultured human nasal epithelial cells, The Journal of allergy and clinical immunology

538   107(2) (2001) 310-4.

539   [10] H. Pavenstadt, W. Kriz, M. Kretzler, Cell biology of the glomerular podocyte, Physiological

540   reviews 83(1) (2003) 253-307.

541 [11] I. Ichikawa, B.M. Brenner, Mechanisms of action of hisamine and histamine antagonists on the

542 glomerular microcirculation in the rat, Circulation research 45(6) (1979) 737-45.

543 [12] D.B. Lee, E. Huang, H.J. Ward, Tight junction biology and kidney dysfunction, American

544 journal of physiology. Renal physiology 290(1) (2006) F20-34.

545 [13] E. Schnabel, J.M. Anderson, M.G. Farquhar, The tight junction protein ZO-1 is concentrated

546 along slit diaphragms of the glomerular epithelium, The Journal of cell biology 111(3) (1990) 1255-

547 63.

548 [14] D.B. Johnstone, L.B. Holzman, Clinical impact of research on the podocyte slit diaphragm,

549 Nature clinical practice. Nephrology 2(5) (2006) 271-82.

550 [15] K. Tryggvason, J. Patrakka, Thin basement membrane nephropathy, Journal of the American

551 Society of Nephrology : JASN 17(3) (2006) 813-22.

552 [16] R. Verma, I. Kovari, A. Soofi, D. Nihalani, K. Patrie, L.B. Holzman, Nephrin ectodomain

553 engagement results in Src kinase activation, nephrin phosphorylation, Nck recruitment, and actin

554 polymerization, The Journal of clinical investigation 116(5) (2006) 1346-59.

555 [17] E. Yaoita, N. Sato, Y. Yoshida, M. Nameta, T. Yamamoto, Cadherin and catenin staining in

556 podocytes in development and puromycin aminonucleoside nephrosis, Nephrology, dialysis,

557 transplantation : official publication of the European Dialysis and Transplant Association -

558 European Renal Association 17 Suppl 9 (2002) 16-9.

559 [18] L.N. Sun, Z.X. Chen, X.C. Liu, H.Y. Liu, G.J. Guan, G. Liu, Curcumin ameliorates epithelial-

560 to-mesenchymal transition of podocytes in vivo and in vitro via regulating caveolin-1, Biomedicine

561 & pharmacotherapy = Biomedecine & pharmacotherapie 68(8) (2014) 1079-88.

562 [19] S.J. Shankland, J.W. Pippin, J. Reiser, P. Mundel, Podocytes in culture: past, present, and

563 future, Kidney international 72(1) (2007) 26-36.

564 [20] P.T. Brinkkoetter, C. Ising, T. Benzing, The role of the podocyte in albumin filtration, Nature

565 reviews. Nephrology 9(6) (2013) 328-36.

566   [21] H.E. Abboud, S.L. Ou, J.A. Velosa, S.V. Shah, T.P. Dousa, Dynamics of renal histamine in

567   normal rat kidney and in nephrosis induced by aminonucleoside of puromycin, The Journal of

568   clinical investigation 69(2) (1982) 327-36.

569   [22] J.R. Sedor, H.E. Abboud, Actions and metabolism of histamine in glomeruli and tubules of the

570   human kidney, Kidney international 26(2) (1984) 144-52.

571   [23] J.R. Sedor, H.E. Abboud, Histamine modulates contraction and cyclic nucleotides in cultured

572   rat mesangial cells. Differential effects mediated by histamine H1 and H2 receptors, The Journal of

573   clinical investigation 75(5) (1985) 1679-89.

574   [24] A.C. Rosa, C. Grange, A. Pini, M.A. Katebe, E. Benetti, M. Collino, G. Miglio, D. Bani, G.

575   Camussi, P.L. Chazot, R. Fantozzi, Overexpression of histamine H(4) receptors in the kidney of

576   diabetic rat, Inflammation research : official journal of the European Histamine Research Society ...

577   [et al.] 62(4) (2013) 357-65.

578   [25] A. Pini, P.L. Chazot, E. Veglia, A. Moggio, A.C. Rosa, H3 receptor renal expression in normal

579   and diabetic rats, Inflammation research : official journal of the European Histamine Research

580   Society ... [et al.] 64(5) (2015) 271-3.

581   [26] E. Veglia, C. Grange, A. Pini, A. Moggio, C. Lanzi, G. Camussi, P.L. Chazot, A.C. Rosa,

582   Histamine receptor expression in human renal tubules: a comparative pharmacological evaluation,

583   Inflammation research : official journal of the European Histamine Research Society ... [et al.]

584   64(3-4) (2015) 261-70.

585   [27] P.G. Conaldi, L. Biancone, A. Bottelli, A. De Martino, G. Camussi, A. Toniolo, Distinct

586   pathogenic effects of group B coxsackieviruses on human glomerular and tubular kidney cells,

587   Journal of virology 71(12) (1997) 9180-7.

588   [28] S. Doublier, V. Ruotsalainen, G. Salvidio, E. Lupia, L. Biancone, P.G. Conaldi, P. Reponen,

589   K. Tryggvason, G. Camussi, Nephrin redistribution on podocytes is a potential mechanism for

590   proteinuria in patients with primary acquired nephrotic syndrome, The American journal of

591   pathology 158(5) (2001) 1723-31.

592 [29] F. Collino, M.C. Deregibus, S. Bruno, L. Sterpone, G. Aghemo, L. Viltono, C. Tetta, G.

593 Camussi, Microvesicles derived from adult human bone marrow and tissue specific mesenchymal

594 stem cells shuttle selected pattern of miRNAs, PloS one 5(7) (2010) e11803.

595 [30] A.S. Awad, M. Rouse, L. Liu, A.L. Vergis, D.L. Rosin, J. Linden, J.R. Sedor, M.D. Okusa,

596 Activation of adenosine 2A receptors preserves structure and function of podocytes, Journal of the

597 American Society of Nephrology : JASN 19(1) (2008) 59-68.

598 [31] M. Dey, A. Baldys, D.B. Sumter, P. Gooz, L.M. Luttrell, J.R. Raymond, M. Gooz, Bradykinin

599 decreases podocyte permeability through ADAM17-dependent epidermal growth factor receptor

600 activation and zonula occludens-1 rearrangement, The Journal of pharmacology and experimental

601 therapeutics 334(3) (2010) 775-83.

602 [32] A.C. Rosa, L. Rattazzi, G. Miglio, M. Collino, R. Fantozzi, Angiotensin II induces tumor

603 necrosis factor-alpha expression and release from cultured human podocytes, Inflammation research

604 : official journal of the European Histamine Research Society ... [et al.] 61(4) (2012) 311-7.

605 [33] R.M. van Rijn, P.L. Chazot, F.C. Shenton, K. Sansuk, R.A. Bakker, R. Leurs, Oligomerization

606 of recombinant and endogenously expressed human histamine H(4) receptors, Mol Pharmacol 70(2)

607 (2006) 604-15.

608 [34] D. Dijkstra, R. Leurs, P. Chazot, F.C. Shenton, H. Stark, T. Werfel, R. Gutzmer, Histamine

609 downregulates monocyte CCL2 production through the histamine H4 receptor, The Journal of

610 allergy and clinical immunology 120(2) (2007) 300-7.

611 [35] W. Baumer, S. Wendorff, R. Gutzmer, T. Werfel, D. Dijkstra, P. Chazot, H. Stark, M.

612 Kietzmann, Histamine H4 receptors modulate dendritic cell migration through skin--

613 immunomodulatory role of histamine, Allergy 63(10) (2008) 1387-94.

614 [36] D. Dijkstra, H. Stark, P.L. Chazot, F.C. Shenton, R. Leurs, T. Werfel, R. Gutzmer, Human

615 inflammatory dendritic epidermal cells express a functional histamine H4 receptor, The Journal of

616 investigative dermatology 128(7) (2008) 1696-703.

617 [37] D. Grandi, F.C. Shenton, P.L. Chazot, G. Morini, Immunolocalization of histamine H3

618 receptors on endocrine cells in the rat gastrointestinal tract, Histology and histopathology 23(7)

619 (2008) 789-98.

620 [38] G. Morini, G. Becchi, F.C. Shenton, P.L. Chazot, D. Grandi, Histamine H3 and H4 receptors

621 are expressed on distinct endocrine cell types in the rat fundic mucosa, Inflammation research :

622 official journal of the European Histamine Research Society ... [et al.] 57 Suppl 1 (2008) S57-8.

623 [39] R.M. van Rijn, A. van Marle, P.L. Chazot, E. Langemeijer, Y. Qin, F.C. Shenton, H.D. Lim,

624 O.P. Zuiderveld, K. Sansuk, M. Dy, M.J. Smit, C.P. Tensen, R.A. Bakker, R. Leurs, Cloning and

625 characterization of dominant negative splice variants of the human histamine H4 receptor, The

626 Biochemical journal 414(1) (2008) 121-31.

627 [40] K. Reidy, K. Susztak, Epithelial-mesenchymal transition and podocyte loss in diabetic kidney

628 disease, American journal of kidney diseases : the official journal of the National Kidney

629 Foundation 54(4) (2009) 590-3.

630 [41] S.P. Adderley, X.E. Zhang, J.W. Breslin, Involvement of the H1 histamine receptor, p38 MAP

631 kinase, MLCK, and Rho/ROCK in histamine-induced endothelial barrier dysfunction,

632 Microcirculation (2015).

633 [42] Q. Zhang, K. Fisher, Tight junction-related barrier contributes to the electrophysiological

634 asymmetry across vocal fold epithelium, PloS one 7(3) (2012) e34017.

635 [43] G. Miglio, A.C. Rosa, L. Rattazzi, C. Grange, M. Collino, G. Camussi, R. Fantozzi, The

636 subtypes of peroxisome proliferator-activated receptors expressed by human podocytes and their

637 role in decreasing podocyte injury, British journal of pharmacology 162(1) (2011) 111-25.

638 [44] G. Miglio, A.C. Rosa, L. Rattazzi, C. Grange, G. Camussi, R. Fantozzi, Protective effects of

639 peroxisome proliferator-activated receptor agonists on human podocytes: proposed mechanisms of

640 action, British journal of pharmacology 167(3) (2012) 641-53.

641 [45] C. Swan, S.A. Richards, N.P. Duroudier, I. Sayers, I.P. Hall, Alternative promoter use and

642 splice variation in the human histamine H1 receptor gene, American journal of respiratory cell and

643 molecular biology 35(1) (2006) 118-26.

644 [46] B.R. Godlewska, L. Olajossy-Hilkesberger, M. Olajossy, J. Limon, J. Landowski,

645 Polymorphisms of the histamine receptor (H1HR) gene are not associated with olanzapine-induced

646 weight gain, Journal of clinical psychopharmacology 33(3) (2013) 436-7.

647 [47] R. Leurs, M.M. Brozius, M.J. Smit, A. Bast, H. Timmerman, Effects of histamine H1-, H2-

648 and H3-receptor selective drugs on the mechanical activity of guinea-pig small and large intestine,

649 British journal of pharmacology 102(1) (1991) 179-85.

650 [48] M. Al-Gadi, S.J. Hill, Characterization of histamine receptors mediating the stimulation of

651 cyclic AMP accumulation in rabbit cerebral cortical slices, British journal of pharmacology 85(4)

652 (1985) 877-88.

653 [49] A.N. Nicholson, P.A. Pascoe, C. Turner, C.R. Ganellin, P.M. Greengrass, A.F. Casy, A.D.

654 Mercer, Sedation and histamine H1-receptor antagonism: studies in man with the enantiomers of

655 chlorpheniramine and dimethindene, British journal of pharmacology 104(1) (1991) 270-6.

656 [50] D.M. Shasby, D.R. Ries, S.S. Shasby, M.C. Winter, Histamine stimulates phosphorylation of

657 adherens junction proteins and alters their link to vimentin, American journal of physiology. Lung

658 cellular and molecular physiology 282(6) (2002) L1330-8.

659 [51] R.A. Budworth, M. Anderson, R.H. Clothier, L. Leach, Histamine-induced Changes in the

660 Actin Cytoskeleton of the Human Microvascular Endothelial Cell line HMEC-1, Toxicology in

661 vitro : an international journal published in association with BIBRA 13(4-5) (1999) 789-95.

662 [52] S.Y. Yuan, Signal transduction pathways in enhanced microvascular permeability,

663 Microcirculation 7(6 Pt 1) (2000) 395-403.

664 [53] C.M. Mikelis, M. Simaan, K. Ando, S. Fukuhara, A. Sakurai, P. Amornphimoltham, A.

665 Masedunskas, R. Weigert, T. Chavakis, R.H. Adams, S. Offermanns, N. Mochizuki, Y. Zheng, J.S.

666 Gutkind, RhoA and ROCK mediate histamine-induced vascular leakage and anaphylactic shock,

667 Nature communications 6 (2015) 6725.

668 [54] S. Hishinuma, J.M. Young, Characteristics of the binding of [3H]-mepyramine to intact human

669 U373 MG astrocytoma cells: evidence for histamine-induced H1-receptor internalisation, British

670 journal of pharmacology 116(6) (1995) 2715-23.

671 [55] S. Beermann, R. Seifert, D. Neumann, Commercially available antibodies against human and

672 murine histamine H(4)-receptor lack specificity, Naunyn-Schmiedeberg's archives of pharmacology

673 385(2) (2012) 125-35.

674 [56] R. Gutzmer, T. Werfel, W. Baumer, M. Kietzmann, P.L. Chazot, R. Leurs, Well characterized

675 antihistamine 4 receptor antibodies contribute to current knowledge of the expression and biology

676 of the human and murine histamine 4 receptor, Naunyn-Schmiedeberg's archives of pharmacology

677 385(9) (2012) 853-4; author reply 855-60.

678 [57] R. Seifert, E.H. Schneider, S. Dove, I. Brunskole, D. Neumann, A. Strasser, A. Buschauer,

679 Paradoxical stimulatory effects of the "standard" histamine H4-receptor antagonist JNJ7777120: the

680 H4 receptor joins the club of 7 transmembrane domain receptors exhibiting functional selectivity,

681 Mol Pharmacol 79(4) (2011) 631-8.

682 [58] J. Reiser, W. Kriz, M. Kretzler, P. Mundel, The glomerular slit diaphragm is a modified

683 adherens junction, Journal of the American Society of Nephrology : JASN 11(1) (2000) 1-8.

684 [59] Y. Li, Y.S. Kang, C. Dai, L.P. Kiss, X. Wen, Y. Liu, Epithelial-to-mesenchymal transition is a

685 potential pathway leading to podocyte dysfunction and proteinuria, The American journal of

686 pathology 172(2) (2008) 299-308.

687 [60] J.C. Sedeyn, H. Wu, R.D. Hobbs, E.C. Levin, R.G. Nagele, V. Venkataraman, Histamine

688 Induces Alzheimer's Disease-Like Blood Brain Barrier Breach and Local Cellular Responses in

689 Mouse Brain Organotypic Cultures, BioMed research international 2015 (2015) 937148.

690 [61] J. Zou, E. Yaoita, Y. Watanabe, Y. Yoshida, M. Nameta, H. Li, Z. Qu, T. Yamamoto,

691 Upregulation of nestin, vimentin, and desmin in rat podocytes in response to injury, Virchows

692 Archiv : an international journal of pathology 448(4) (2006) 485-92.

693 [62] C.B. Wilson, L.C. Gushwa, O.W. Peterson, B.J. Tucker, R.C. Blantz, Glomerular immune

694 injury in the rat: effect of antagonists of histamine activity, Kidney international 20(5) (1981) 628-

695 35.

696
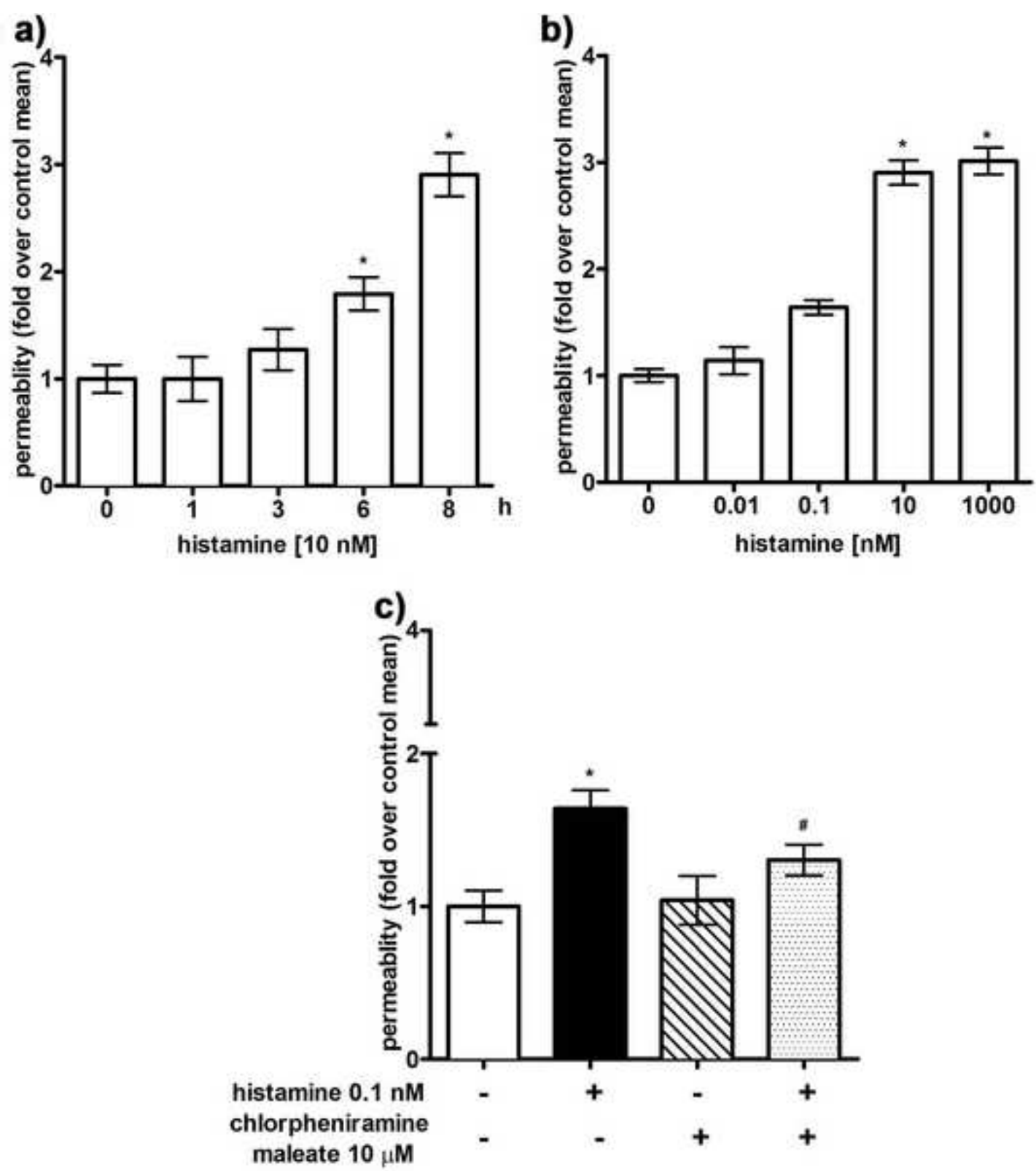
a) control   histamine 10 nM

chlorpheniramine 10 µM   chlorpheniramine + histamine

b)

intercellular space width (n of pixel)

histamine 0.1 nM	−	+	−	+
chlorpheniramine maleate 10 µM	−	−	+	+

a)

b)

c)
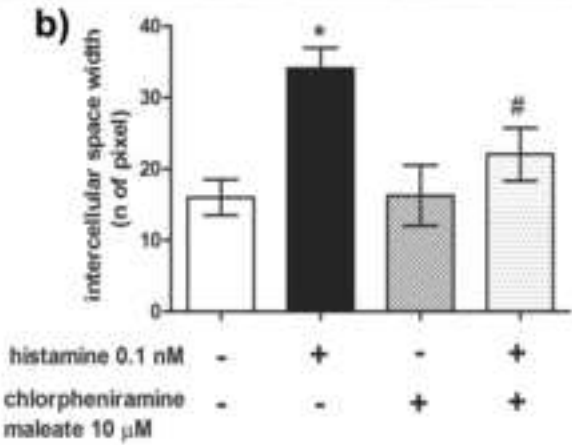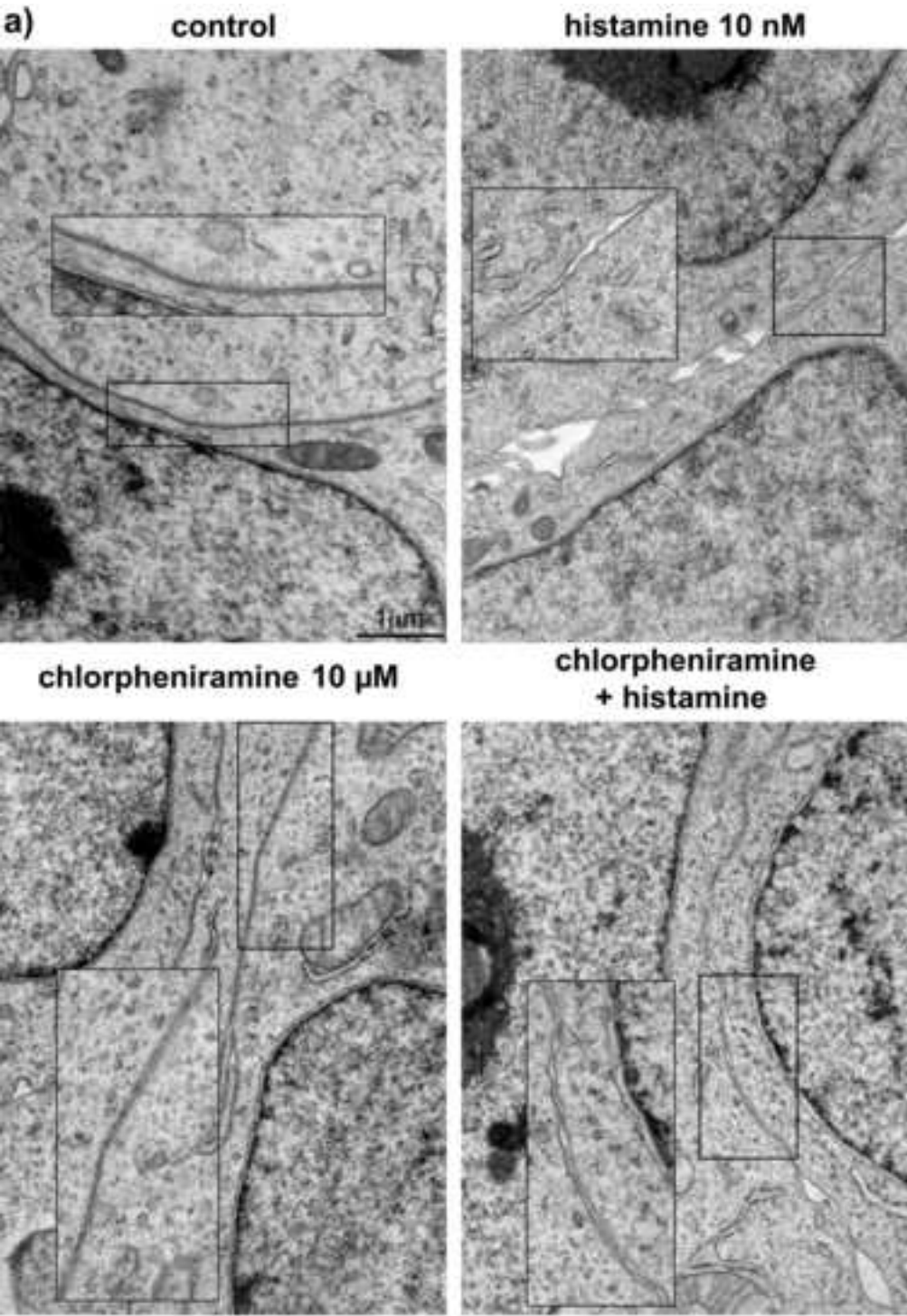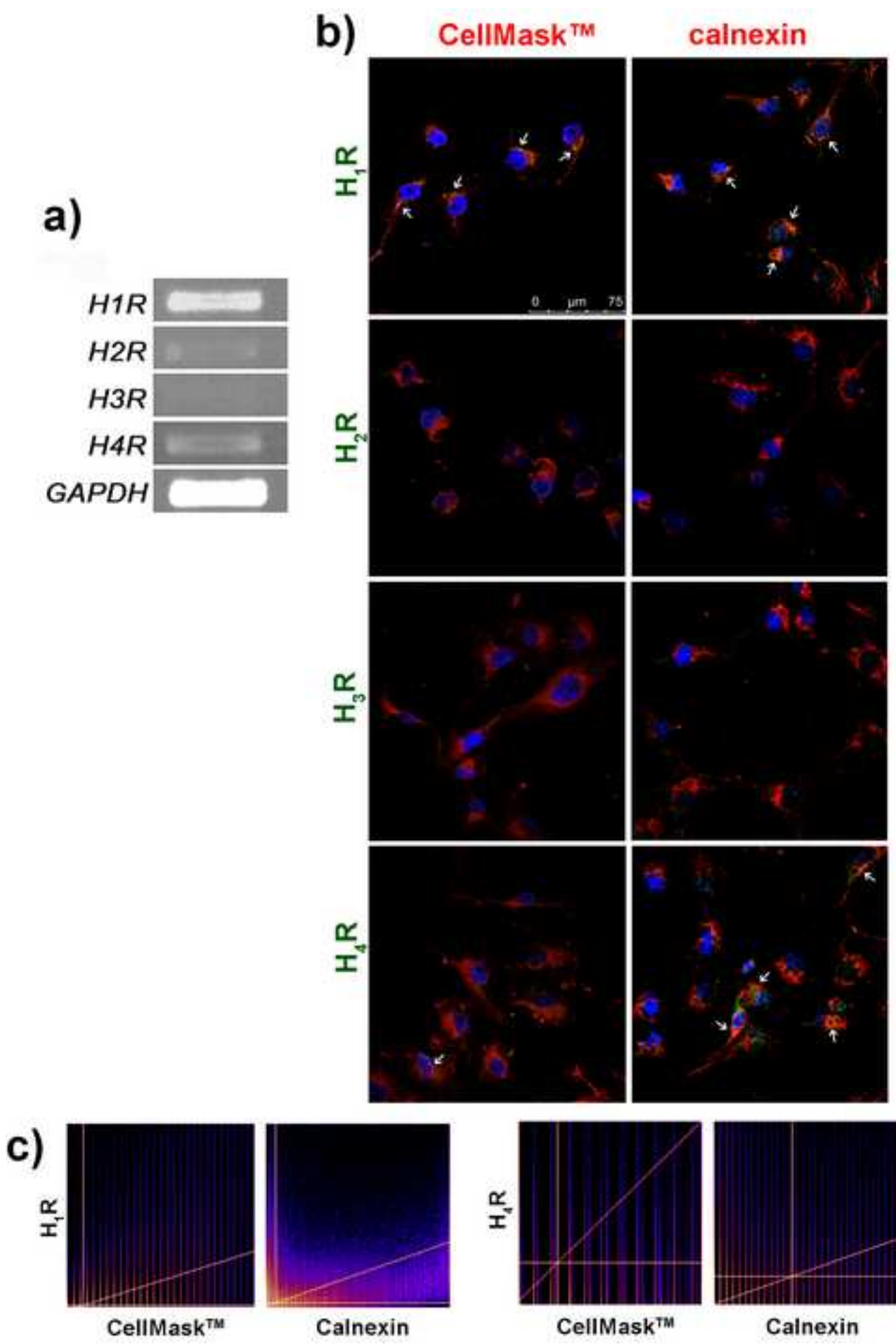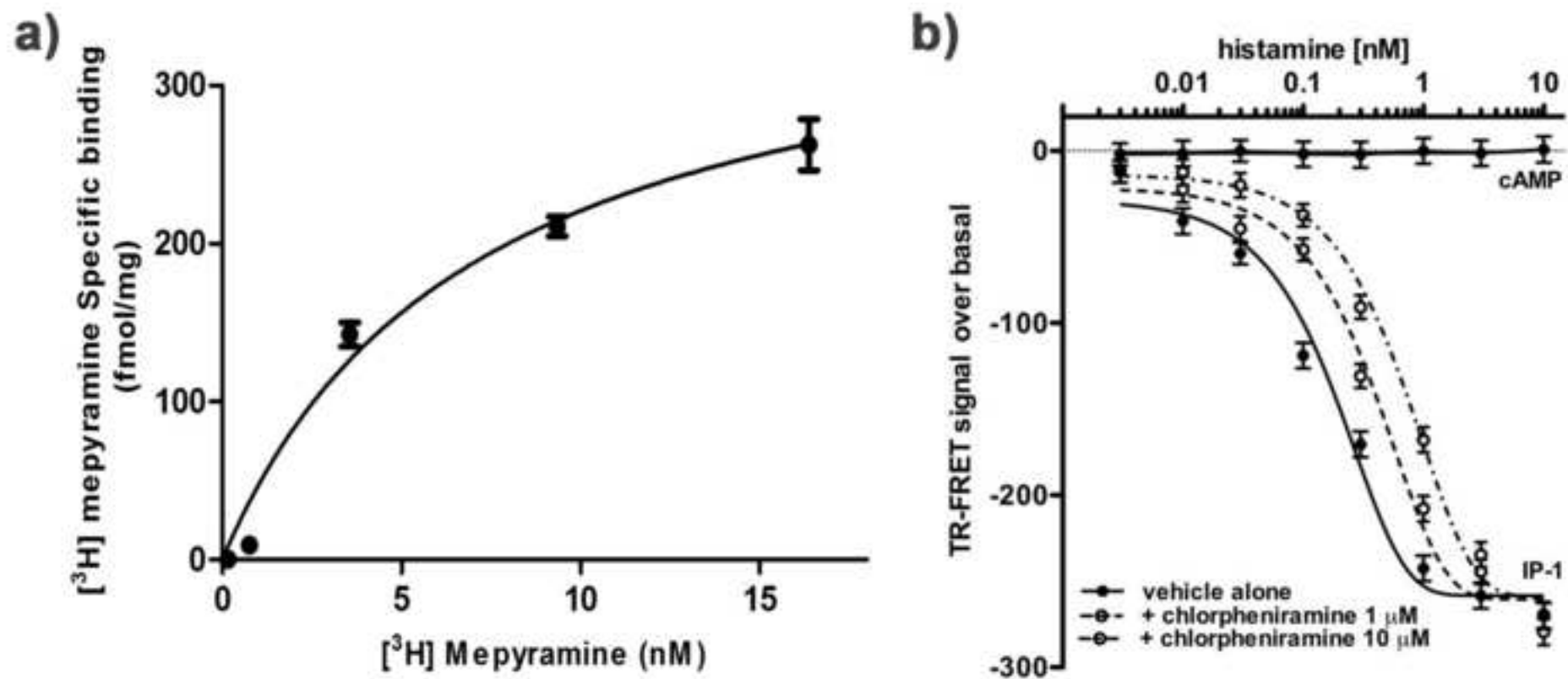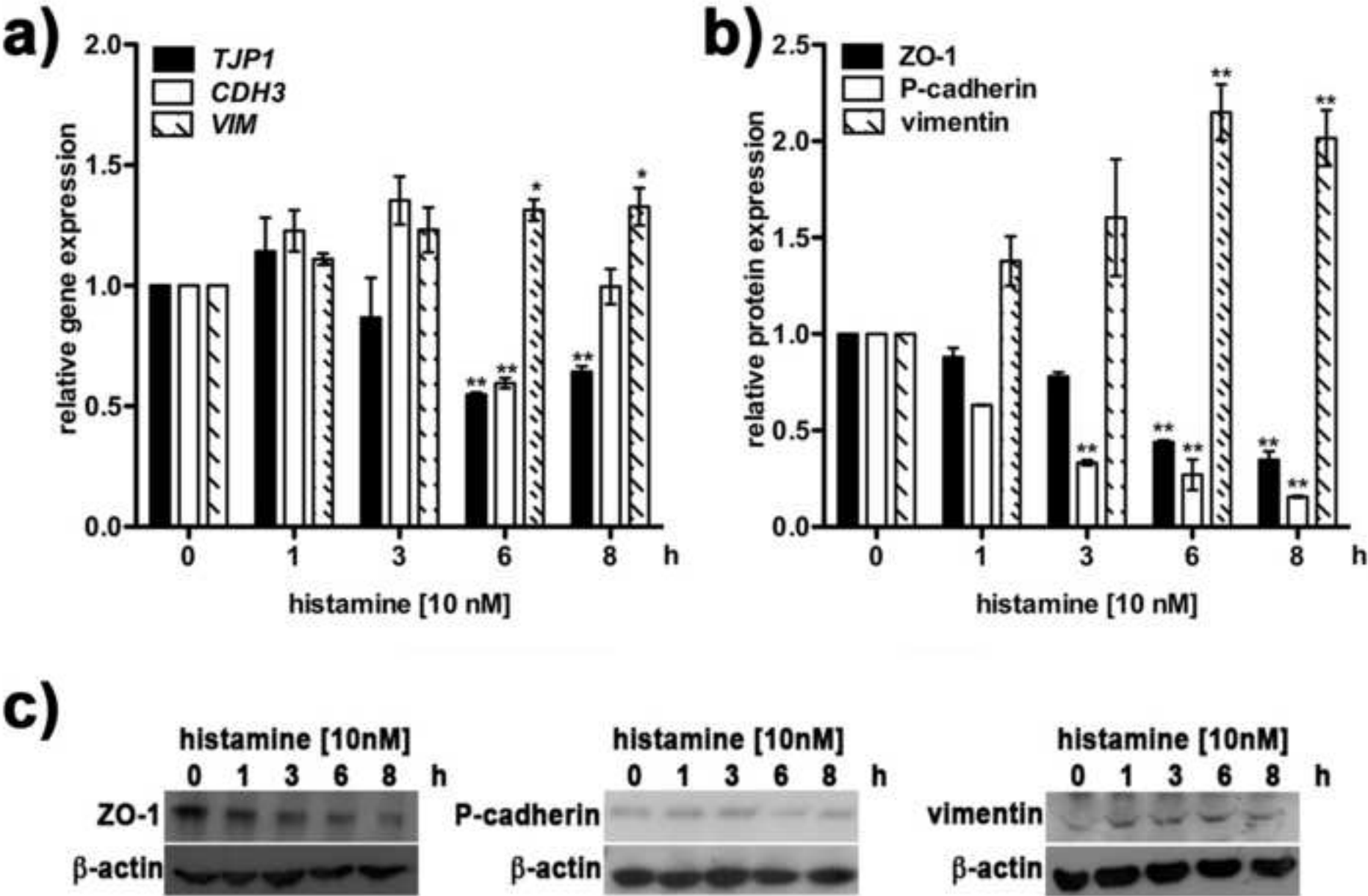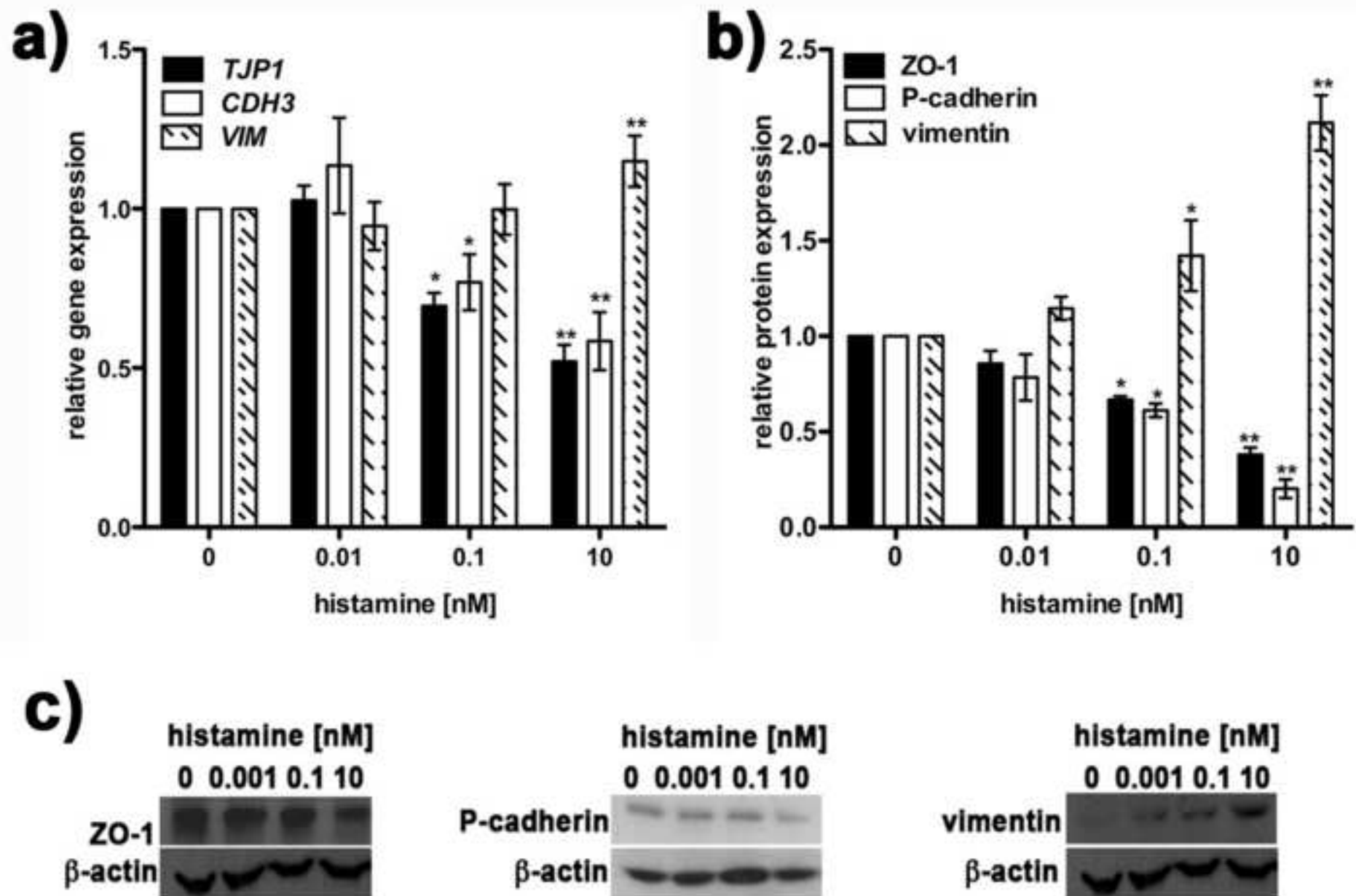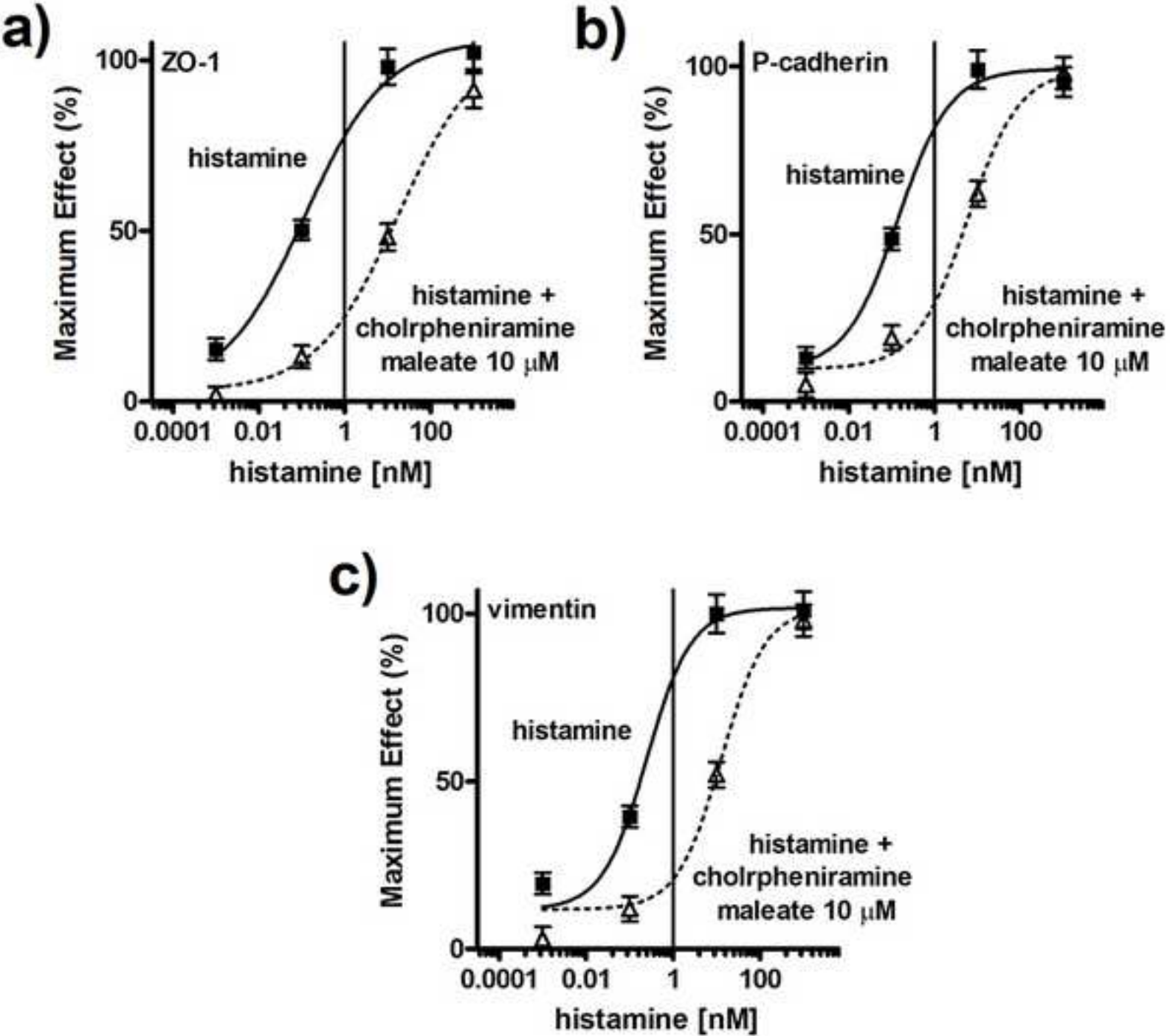
List of chemical compounds studied in the article

1. [^{3}H]mepyramine PubChem CID 656400

2. Chlorpheniramine maleate PubChem CID 5281068

3. Difenhydramine Pubmed CID 3100

4. Histamine dihydrochloride PubChem CID 5818

Supplementary Material - Materials and Methods

Immunocytofluorescence and confocal analysis

Podocytes plated on collagen-coated cover glasses treated with vehicle alone or histamine 10 nM for 0-8 h, were fixed with 4% paraformaldehyde for 10 minutes at room temperature. Sections were incubated overnight with goat polyclonal anti-synaptopodin 1.3 µg/ml (N14, sc-21536), rabbit anti-podocin 2 µg/ml (H130, sc-21009), goat anti-rabbit H_4R 2 µg/ml (Y19 sc-33967; Santa Cruz Biotechnology Inc., Dallas, TX, USA), or rabbit polyclonal anti-HDC 0.4 µg/ml (HPA038891; Sigma–Aldrich St. Louis, MO) at 4°C. After incubation with the respective Alexa-Conjugated secondary antibodies the nuclei were stained with Hoescht. All the slides were examined at ×63 magnification using the SP5 Confocal Laser Scanning Microscope SMD (Leica). A variable number of optical section images in the z-dimension (z-spacing, 0.42 µm) were collected ensuring that images throughout the 3D cellular structure, spanning multiple confocal planes, were fully captured.

Fluorometric quantification of histamine

Podocytes seeded at a density of 800.000 cell/ml were pelleted after one hour from medium re-challenge and the medium was collected. Both pellet and medium were processed accordingly to the standard fluorimetric protocol reported in the Histamine Methods & Tools Database (https://www.i-med.ac.at/hmtd/) for the quantification of histamine. Histmaine extracted in *n*-butanol was reconstituted in aqueous phase using 0.1 N sulphuric acid and *n*-heptane and assayed fluorometrically at 360 nm excitation (Tiligada E, et al. Pharmacol Res 2000).
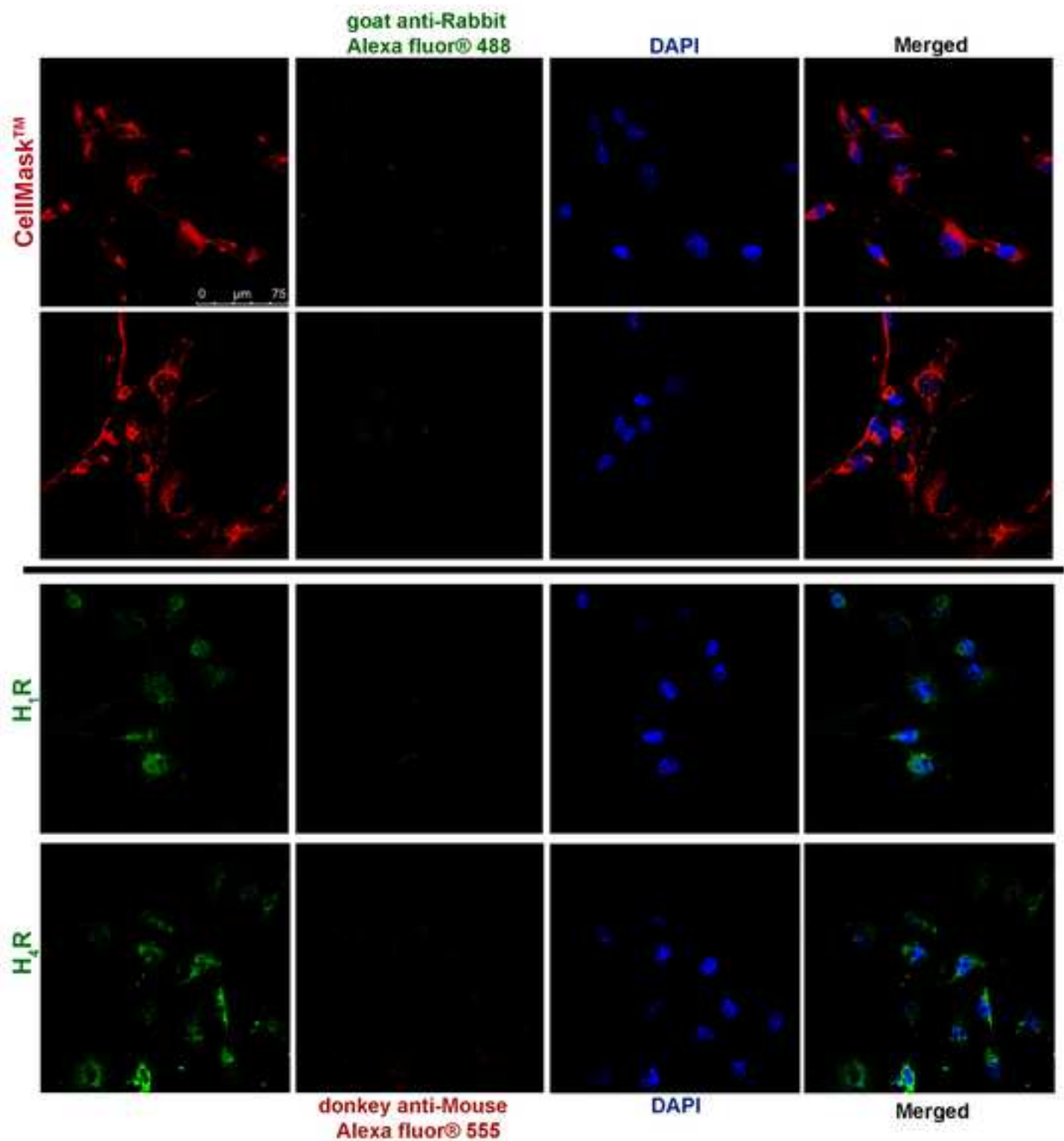
Supplementary Material Fig. 1. Nonspecific binding of the secondary antibodies in colocalization experiments. Representative maximum projection of podocyte Z sections showing the interactions between the different antibodies used. All the slides were examined at ×63 magnification using the SP5 Confocal Laser Scanning Microscope SMD (Leica).
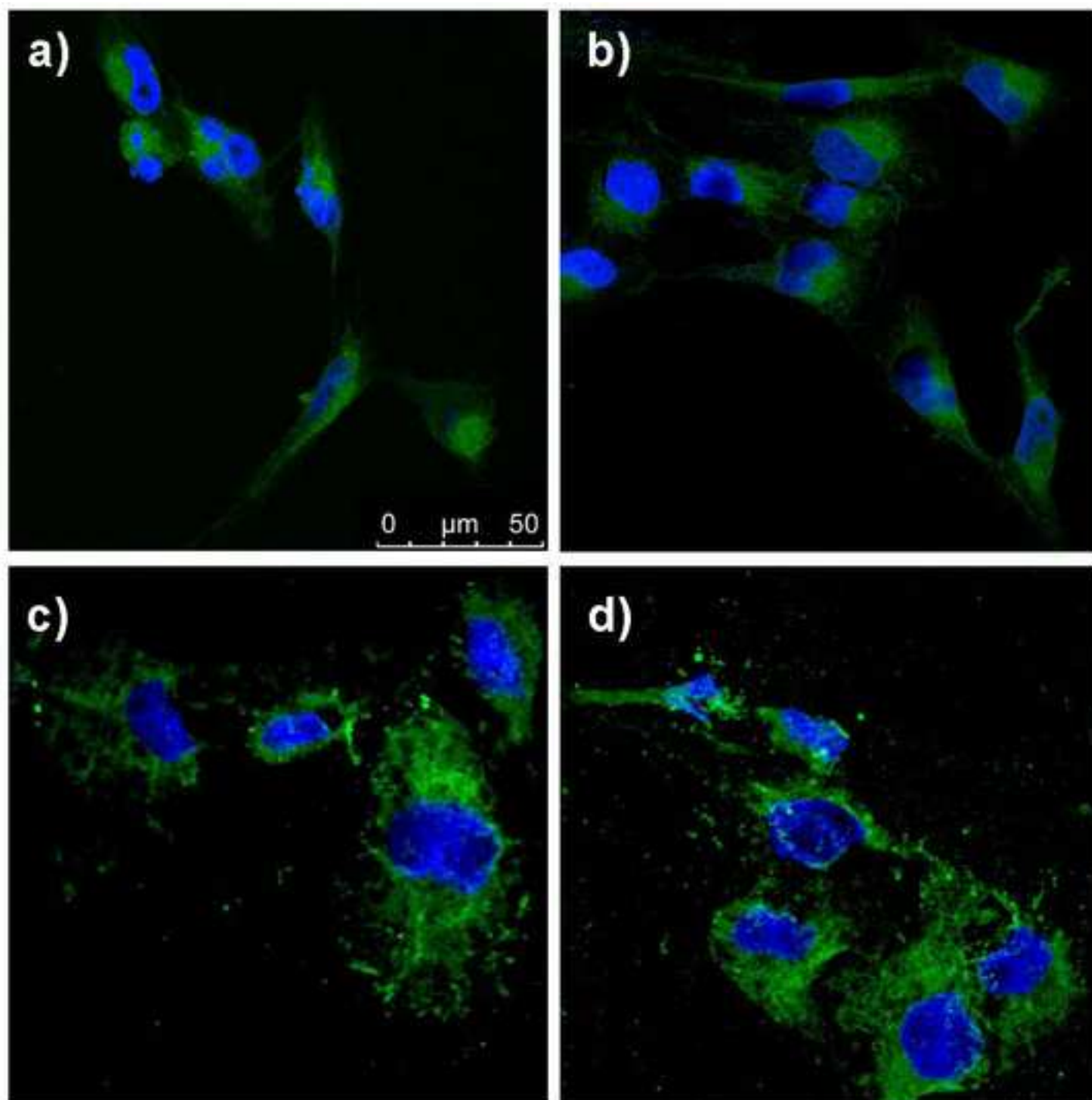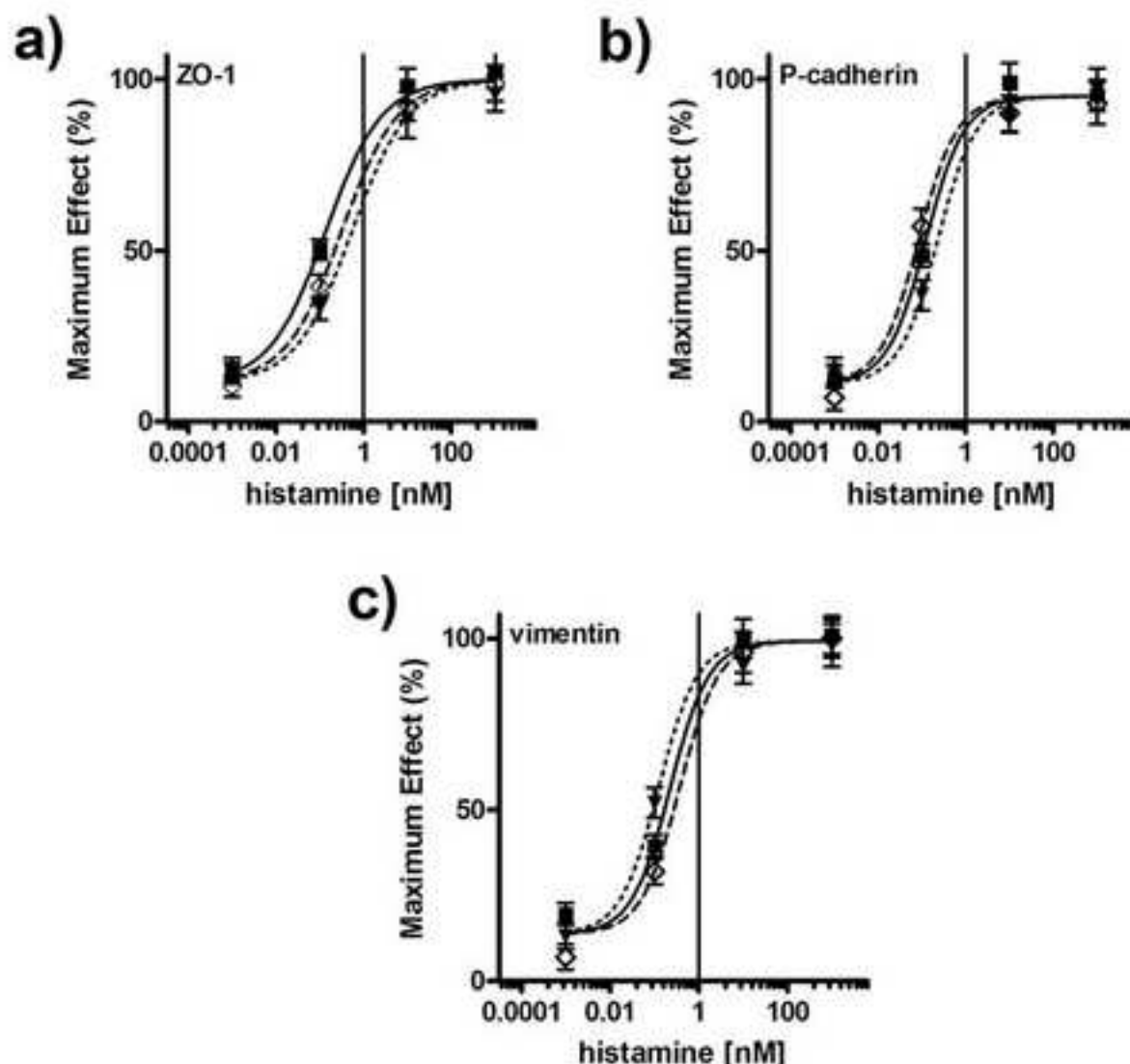
Supplementary Material Fig. 2. Synaptopodin and podocin expression in human immortalized podocytes. Representative maximum projection of the Z sections from 3 independent experiments where cells treated with histamine 10 nM for 0 (a) or 8 (b) h were labelled with specific anti-synaptopodin (a) and (b) or (c) and (d) anti-podocin antibody (green). Nuclei were stained with Hoescht (blue). All the slides were examined at ×63 magnification using the SP5 Confocal Laser Scanning Microscope SMD (Leica).
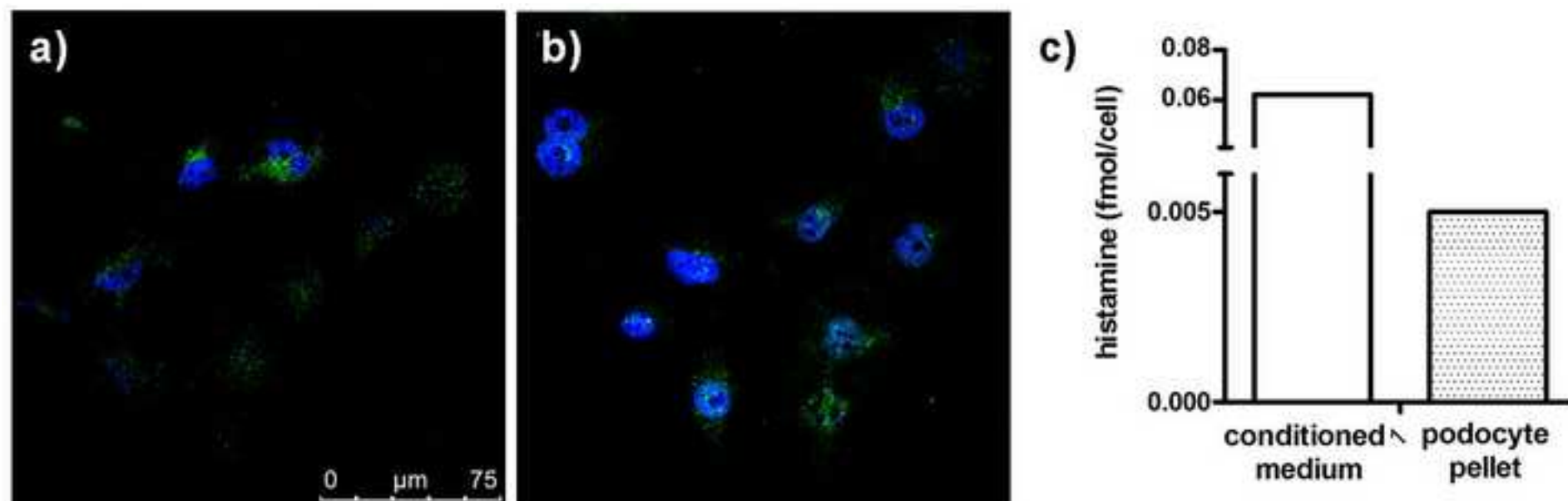
Supplementary Material Fig. 3. **HDC expression and histamine production in human immortalized podocytes.** Representative maximum projection of the Z sections from 3 independent experiments where cells treated with histamine 10 nM for 0 (**a**) or 8 (**b**) h were labelled with the specific anti-HDC antibody (green). Nuclei were stained with Hoescht (blue). All the slides were examined at ×63 magnification using the SP5 Confocal Laser 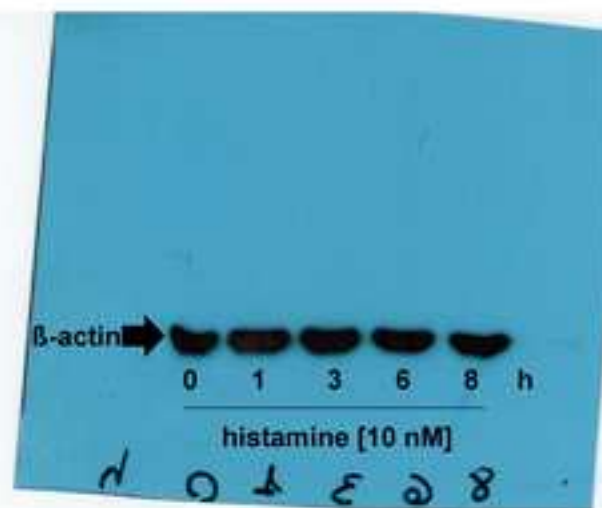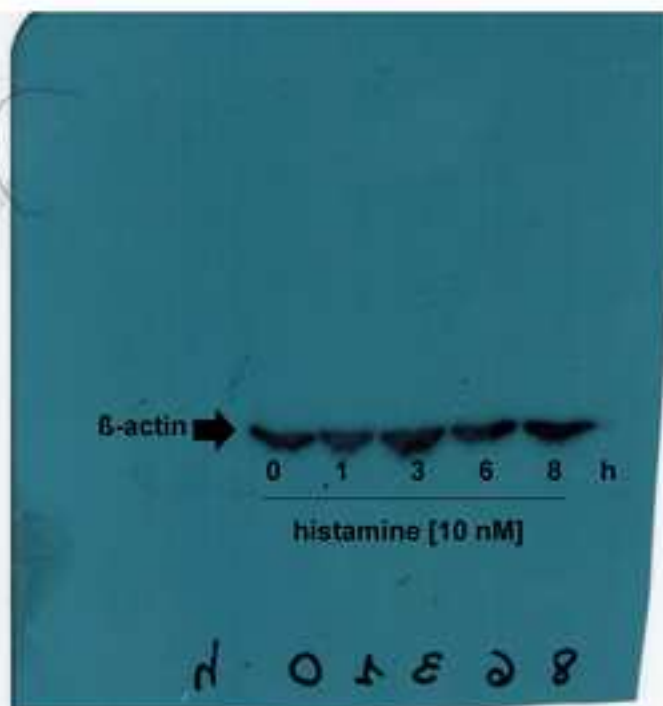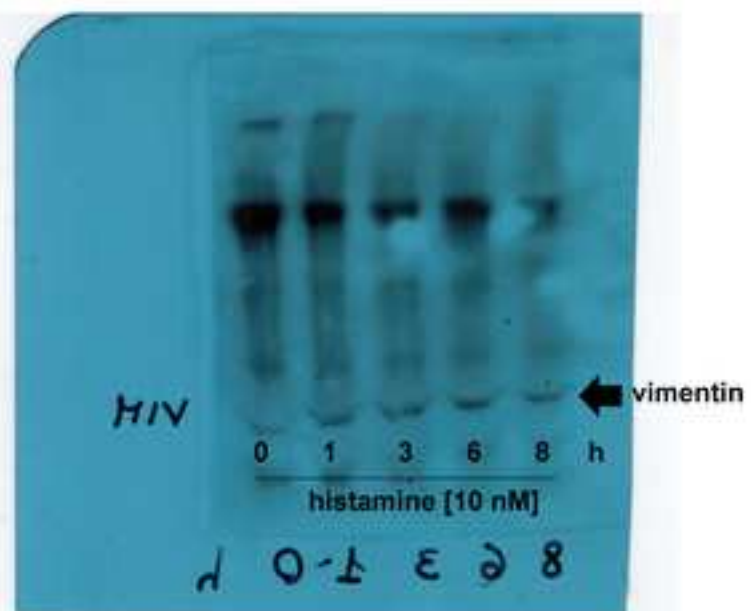Scanning Microscope SMD (Leica). Histamine basal production was measured in two indipendent experiments after 1h of medium rechellenge in both the conditioned medium and the podocyte pellet accordingly to the fluorometric quantification method (**c**).
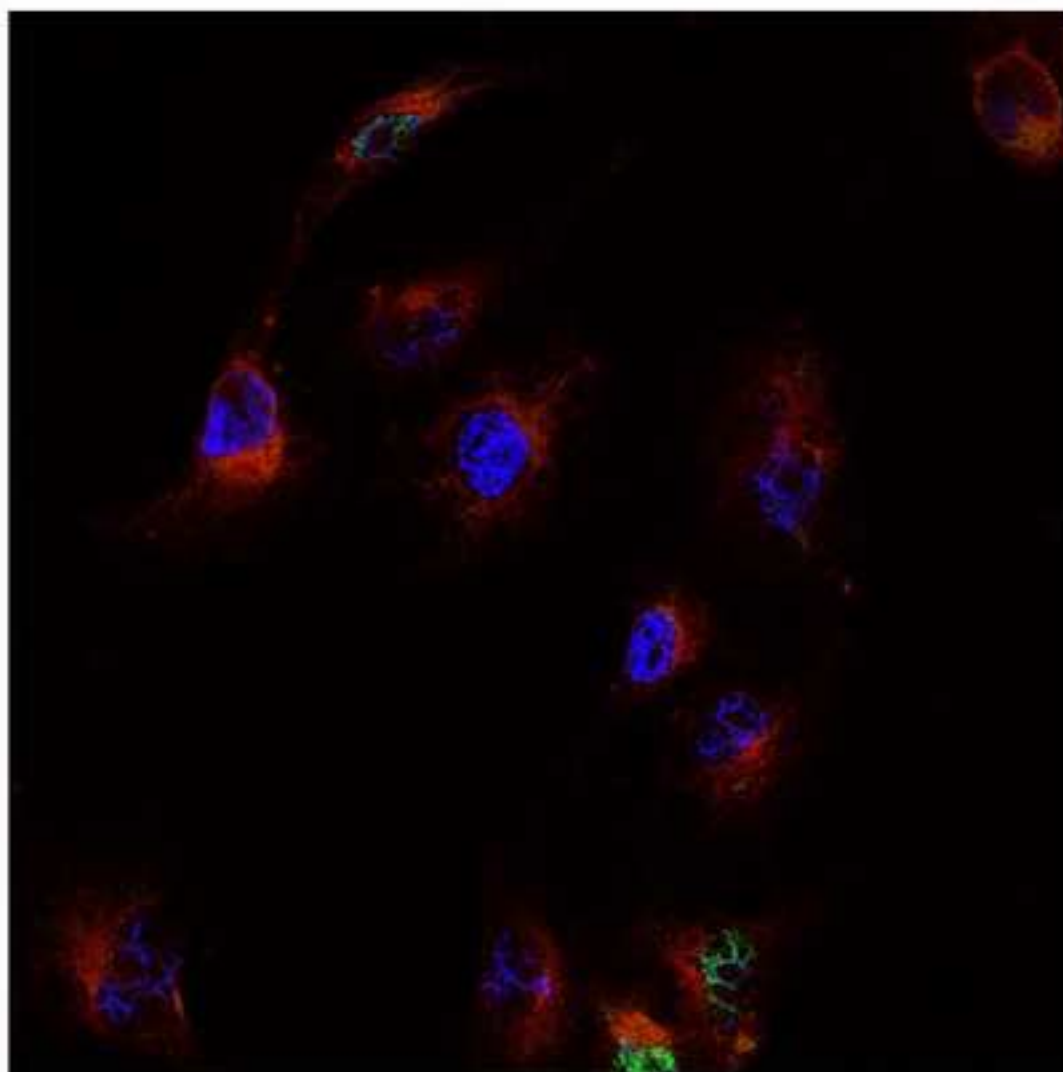
Supplementary Material Fig. 4. H$_4$R expression on human immortalized podocyte plasma membrane. Representative maximum projection of the Z sections from 3 independent experiments where cells were labelled with the Santa Cruz anti-H$_4$R antibody (Y19, sc-33967; green). and CellMask™ Plasma Membrane Stains (red). Nuclei were stained with Hoescht (blue). All the slides were examined at ×63 magnification using the SP5 Confocal Laser Scanning Microscope SMD (Leica).
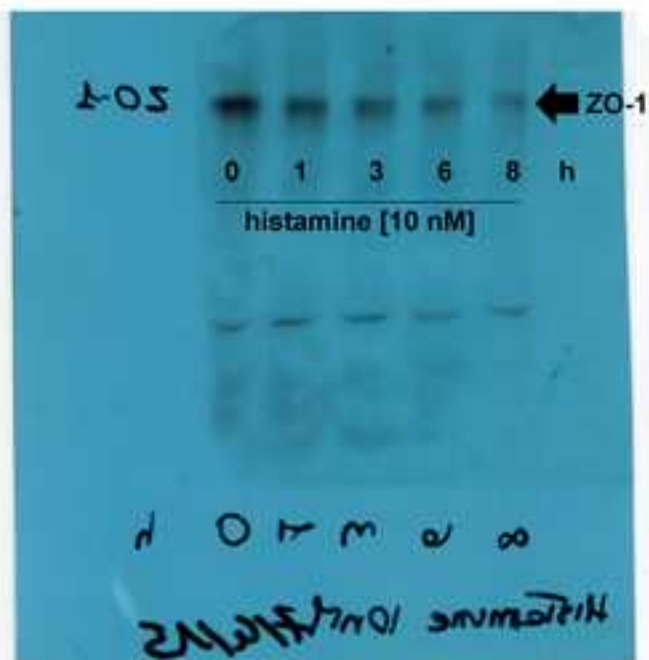
Supplementary Material Fig. 5 Ranitidine and JNJ7777120 antagonism on ZO-1, P-cadherin and vimentin expression evoked by histamine. Human immortalized podocytes pretreated for 10 min with vehicle alone (black square, straight line) or ranitidine (selective H_2R antagonist; black triangle, dotted line) or JNJ7777120 (selective H_4R antagonist; white rhombus, dashed line) 10 µM were treated with histamine for 8 h and processed for ZO-1 (a), P-cadherin (b) and vimentin (c) protein expression. Results, represented as best-fit dose-response curve, are expressed as mean ± SEM of 5 different experiments.
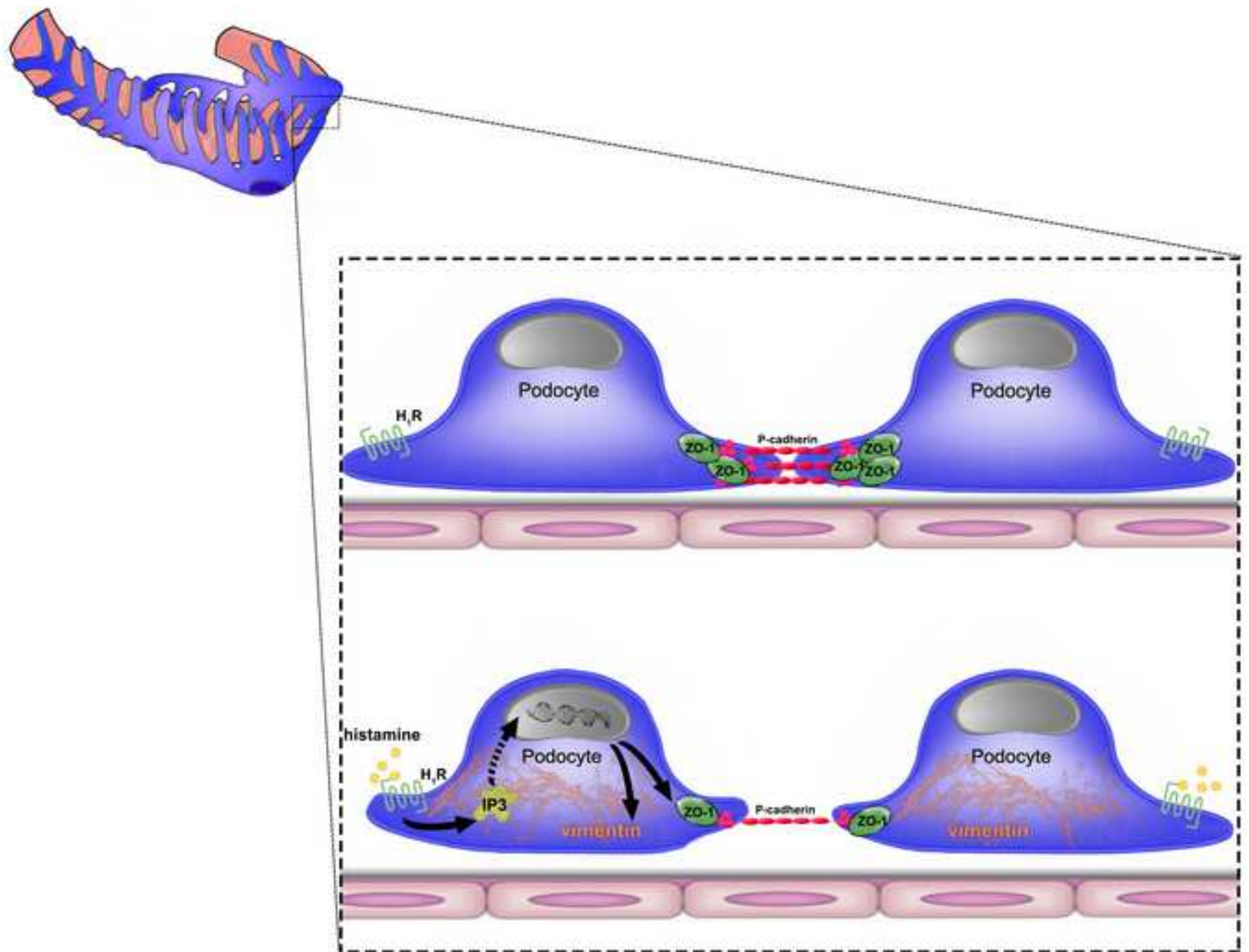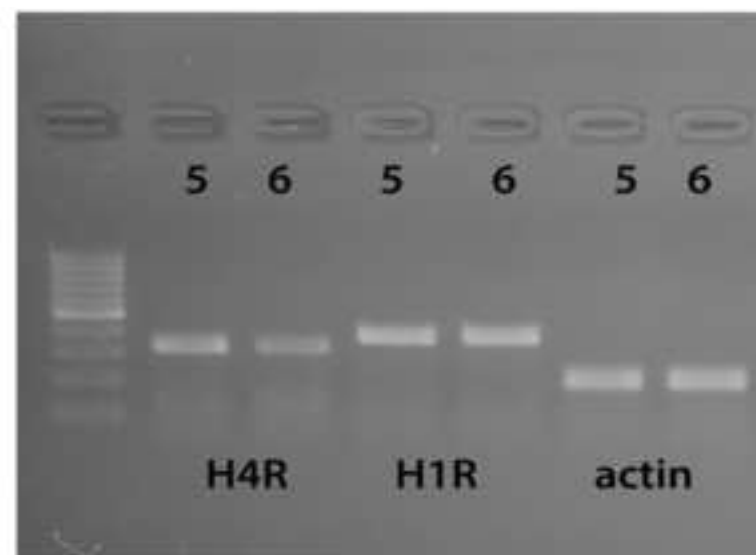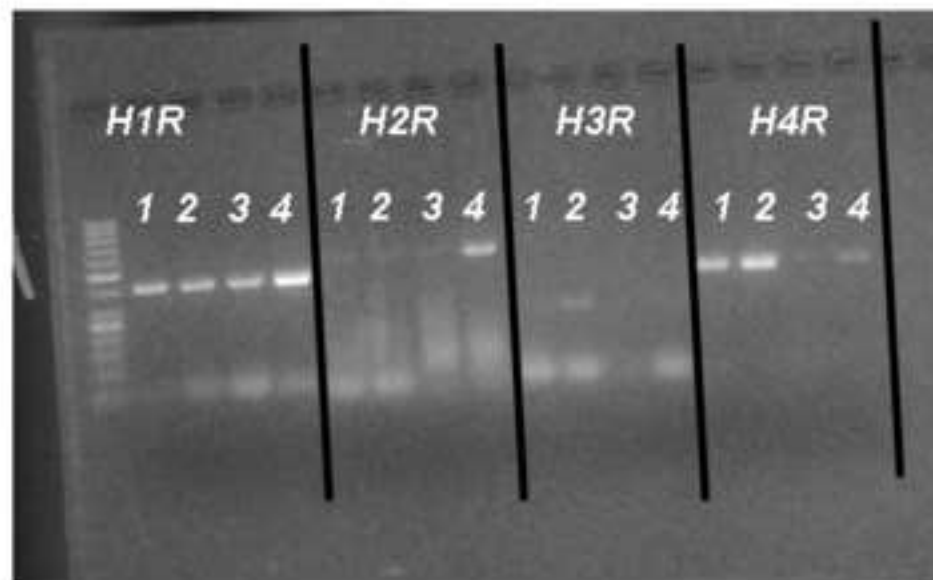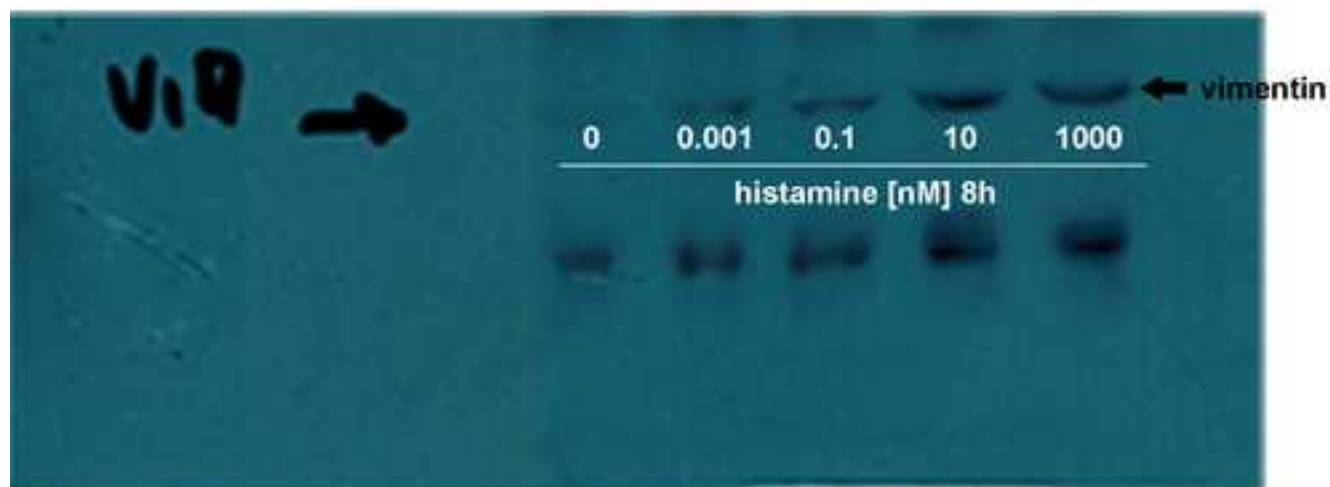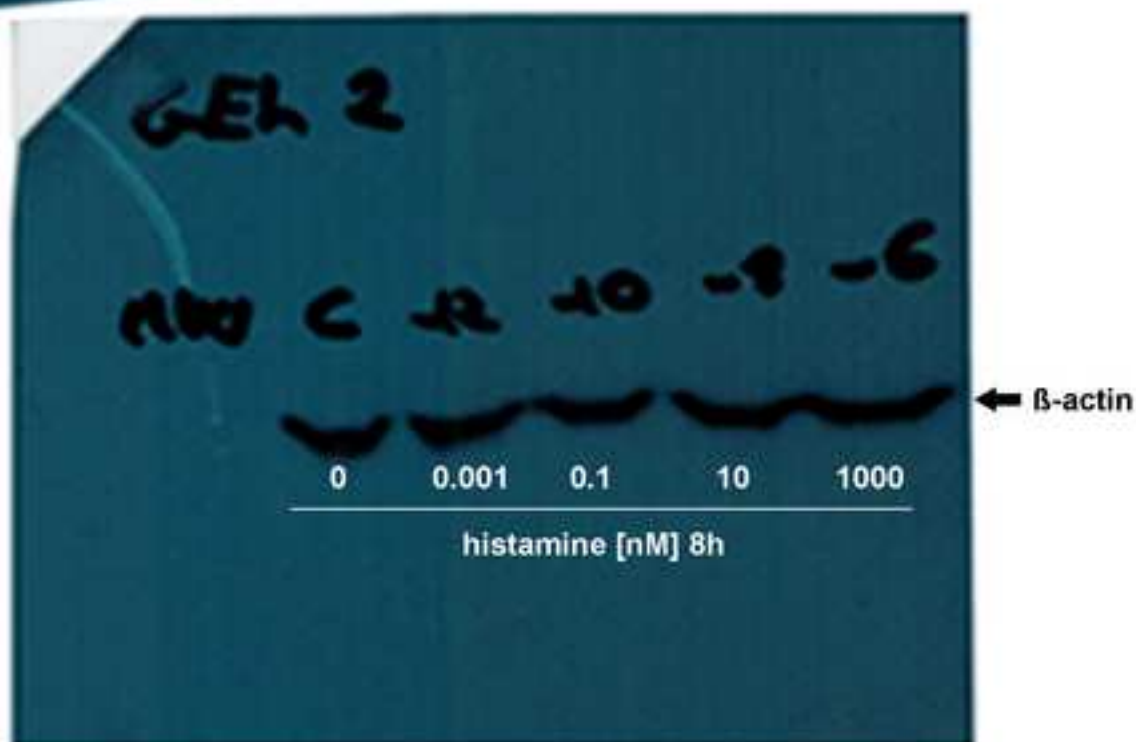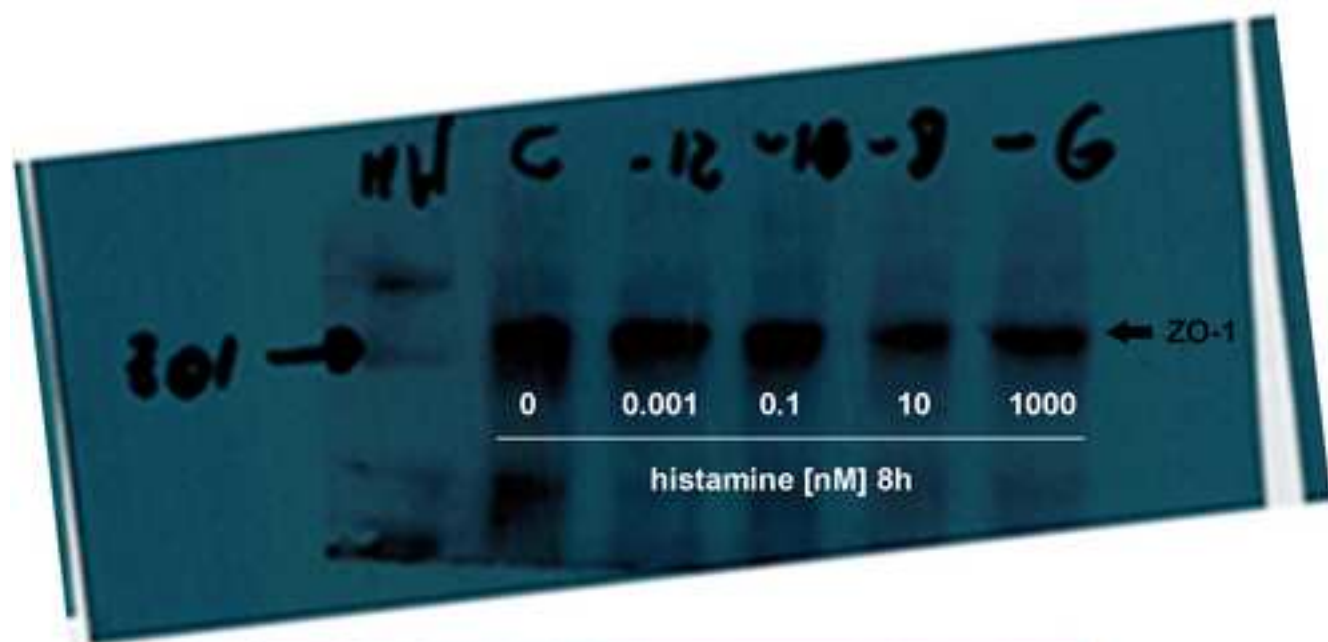
1, 3, 5 and 6 = podocytes
2 and 4 = Tubular epithelial cells
(used as positive control on the basis of
our previous data, Veglia et al., 2015)

ZO-1

0   0.001   0.1   10   1000

histamine [nM] 8h

GEL 2

ß-actin

0   0.001   0.1   10   1000

histamine [nM] 8h

vimentin

0   0.001   0.1   10   1000

histamine [nM] 8h

Conflicts of Interest Statement ————————————

Manuscript title: ————————————————————————————

Uncontrolled Histamine Type 1-Receptor activation of podocytes affects human Glomerular Slit Diaphragm Integrity

————————————————————————————————————

The authors whose names are listed immediately below certify that they have NO affiliations with or involvement in any organization or entity with any financial interest (such as honoraria; educational grants; participation in speakers' bureaus; membership, employment, consultancies, stock ownership, or other equity interest; and expert testimony or patent-licensing arrangements), or non-financial interest (such as personal or professional relationships, affiliations, knowledge or beliefs) in the subject matter or materials discussed in this manuscript.

Author names:

Eleonora Veglia, Alessandro Pini, Aldo Moggio, Cristina Grange, Federica Premoselli, Gianluca Miglio, Ekaterina Tiligada, Roberto Fantozzi, Paul L. Chazot, Arianna Carolina Rosa

The authors whose names are listed immediately below report the following details of affiliation or involvement in an organization or entity with a financial or non-financial interest in the subject matter or materials discussed in this manuscript. Please specify the nature of the conflict on a separate sheet of paper if the space below is inadequate.

Author names:

This statement is signed by all the authors to indicate agreement that the above information is true and correct (a photocopy of this form may be used if there are more than 10 authors):

Author's name (typed)	Author's signature	Date
Eleonora Veglia		01-08-2016
Alessandro Pini		01-08-2016
Aldo Moggio		01-08-2016
Cristina Grange		01-08-2016
Federica Premoselli		01-08-2016
Roberto Fantozzi		01-08-2016
Paul L Chazot		01-08-2016
Arianna Carolina Rosa		01-08-2016
Etiligada Katerina		01-08-2016
Gianluca Miglio		11-10-2016